

THE ROLE OF PRP4K AS A TUMOR SUPPRESSOR IN LEWIS LUNG
CARCINOMA CELLS

by

Carter VanInderstine

Submitted in partial fulfilment of the requirements
for the degree of Master of Science

at

Dalhousie University
Halifax, Nova Scotia
March 2020

© Copyright by Carter VanInderstine, 2020

Table of Contents

| | |
|---|------|
| List of Tables | v |
| List of Figures | vi |
| Abstract | vii |
| List of Abbreviations | viii |
| Acknowledgements | xi |
| Chapter 1: Introduction | 1 |
| 1.1 Cancer | 1 |
| 1.2 Lung Cancer | 3 |
| <i>1.2.1 Introduction</i> | 3 |
| <i>1.2.2 Immunology</i> | 4 |
| <i>1.2.3 Therapies</i> | 5 |
| 1.3 Cancer Stem Cells | 9 |
| <i>1.3.1 Introduction</i> | 9 |
| <i>1.3.2 Identification</i> | 10 |
| <i>1.3.3 Origins</i> | 10 |
| <i>1.3.4 Relationship with Epithelial-to-Mesenchymal Transition</i> | 10 |
| 1.4 Lung Cancer Stem Cells | 14 |
| <i>1.4.1 Introduction</i> | 14 |
| <i>1.4.2 Aldehyde Dehydrogenases</i> | 14 |

| | |
|--|-----------|
| 1.4.3 CD44 | 15 |
| 1.4.4 Hyaluronic Acid..... | 16 |
| 1.5 Pre-mRNA Splicing Factor 4 Kinase (PRP4K) | 17 |
| 1.6 Rationale/ Hypothesis..... | 21 |
| Chapter 2: Methods..... | 22 |
| 2.1 Cell lines and Cell Culture | 22 |
| 2.2 Generation of PRP4K Lentiviral Knockdowns..... | 22 |
| 2.3 Western Blots | 25 |
| 2.4 Immunofluorescence Microscopy | 27 |
| 2.5 ALDEFluor Assays..... | 27 |
| 2.6 Flow Cytometry..... | 28 |
| 2.7 RT-qPCR..... | 28 |
| 2.8 Anoikis Assays | 31 |
| 2.9 Transwell Assays..... | 31 |
| 2.10 Tumorsphere Assays | 32 |
| 2.11 Proliferation Assays | 32 |
| 2.12 Animal Experiments..... | 32 |
| 2.13 Clonogenic Assay..... | 33 |
| 2.14 Statistics | 35 |
| Chapter 3: Results | 36 |

| | |
|--|-----------|
| 3.1 Depletion of PRP4K by shRNA Induces Features of Cancer Stem Cells in the Mouse Lewis Lung Carcinoma Model | 36 |
| 3.2 Feature of Epithelial-to-Mesenchymal transition (EMT) are Associated With Depletion of PRP4K in the Mouse Lewis Lung Carcinoma Model..... | 45 |
| 3.3 PRP4K Knockdown Promotes RA Resistance | 47 |
| 3.4 PRP4K Knockdown Increases Tumor Growth <i>in vivo</i> in the Mouse Lewis Lung Carcinoma Model..... | 51 |
| Chapter 4: Discussion..... | 54 |
| 4.1 Evidence of PRP4K as a Tumor Suppressor..... | 54 |
| 4.2 Stemness | 55 |
| 4.3 Hyaluronic Acid | 57 |
| 4.4 EMT..... | 57 |
| 4.5 Retinoic Acid | 59 |
| 4.6 Limitations..... | 60 |
| Chapter 5: Conclusions | 63 |
| References | 65 |
| Appendix 1..... | 78 |
| Appendix 2..... | 79 |

List of Tables

| | |
|--|----|
| Table 1. Plasmids used in this study | 23 |
| Table 2. Primary and secondary antibodies used in this study..... | 26 |
| Table 3. Primers used in this study | 30 |

List of Figures

| | |
|--|-------------------------------------|
| Figure 1.1 Lung cancer classification by histology and driver mutation breakdown..... | 8 |
| Figure 1.2 Relationship between stemness and EMT progression..... | Error! Bookmark not defined. |
| Figure 1.3 Protein Structure of PRP4K..... | 20 |
| Figure 2.1 Location of processed shRNA binding on the mouse PRP4K transcript beginning with exon one (left) and ending with exon 15 (right). Clone 1 binds the transcript at bases 1375-1388 and Clone 2 binds bases 809-816..... | 24 |
| Figure 2.2 Experimental design for in vivo experiments..... | 34 |
| Figure 3.1 Low PRP4K predicts worse overall survival in lung adenocarcinoma patients..... | 39 |
| Figure 3.2 Validation of PRP4K knockdown in Lewis Lung Carcinoma cells (LLCs) ... | 40 |
| Figure 3.3 Knocking down PRP4K results in increased tumorsphere formation..... | 41 |
| Figure 3.4 PRP4K knockdown does not affect the ALDH or CD44 CSC populations in LLCs..... | 42 |
| Figure 3.5 Further analysis of CSC markers in LLCs..... | 43 |
| Figure 3.6 PRP4K Knockdown exerts its effects in part through hyaluronic acid..... | 44 |
| Figure 3.7 Knockdown of PRP4K affects levels of EMT-related genes in LLCs..... | 46 |
| Figure 3.8 PRP4K Knockdown reduces sensitivity to RA-induced differentiation and gene expression induction in LLCs..... | 48 |
| Figure 3.9 PRP4K knockdown reduces sensitivity to RA-induced proliferation inhibition in LLCs..... | 49 |
| Figure 3.10 PRP4K Knockdown decreases the expression of RA binding proteins in LLCs..... | 50 |
| Figure 3.11 PRP4K knockdown affects tumor growth and metastasis <i>in vivo</i> | 52 |
| Figure 3.12 PRP4K knockdown affected tumor growth but not overall survival in C57BL/6 mice..... | 53 |
| Figure 6.1 Graphical summary of the major findings from the current study..... | 64 |

Abstract

Most patients with lung cancer are diagnosed at late stages when the cancer has spread by metastasis, which is one reason why the five-year survival rate is approximately 14-20%. Although originally identified as a splicing kinase, recent data indicates that pre-mRNA processing factor kinase 4 (PRP4K) may promote metastasis by a partial epithelial-to-mesenchymal transition (EMT) phenotype, and my analysis of PRP4K mRNA levels in 504 lung adenocarcinoma tumors indicates that low PRP4K expression was significantly correlated with worse overall survival. Thus, the objective of this project was to determine the effects of PRP4K loss on lung cancer progression and metastasis *in vivo*. In this thesis, I further characterized the role of PRP4K as a tumor suppressor and showed that knockdown of PRP4K (PRP4K KD) results in a stem-like phenotype in lung adenocarcinoma cells (LLCs) both *in vitro* and *in vivo*. I also found that PRP4K KD resulted in a partial EMT phenotype and resulted in decreased sensitivity to the cancer stem cell targeting compound retinoic acid (RA). I further found that PRP4K KD may induce its phenotype by modulating hyaluronic acid synthesis in these cells. Taken together, these data support the hypothesis that PRP4K is acting a tumor suppressor in lung cancer cells both *in vitro* as well as *in vivo*.

List of Abbreviations Used

4-OHT 4-Hydroxytamoxifen

7-AAD 7-Aminoactinomycin D

ABC ATP Binding Cassette

AID Auxin-Inducible Degron

ALDH Aldehyde Dehydrogenase

ATP Adenosine Triphosphate

bFGF Basic Fibroblast Growth Factor

CD Cluster of Differentiation

CDH1 Cadherin-1 (E-Cadherin)

CDH2 Cadherin-2 (N-Cadherin)

CIC Cancer Initiating Cell

CSC Cancer Stem Cell

DAPI 4',6-diamidino-2-phenylindole

DMEM Dulbecco's Modified Eagle Medium

DNA Deoxyribonucleic Acid

ECL Enhanced Chemiluminescence

EGF Epidermal Growth Factor

EGFR Epidermal Growth Factor Receptor

EMT Epithelial-to-Mesenchymal Transition

FITC Fluorescein isothiocyanate

FBS Fetal bovine serum

GFP Green Fluorescent Protein

HA Hyaluronic Acid

HAS Hyaluronic Acid Synthase

HDAC Histone Deacetylase Complex

HMW High Molecular Weight

HRP Horseradish peroxidase

HYAL Hyaluronidase

IFN Interferon

JAK Janus Kinase

KKHK Lysine-Histidine Rich

LCSC Lung Cancer Stem Cells

LMW Low Molecular Weight

LLC Lewis Lung Carcinoma

LUAD Lung Adenocarcinoma

LUSC Lung Squamous Cell Carcinoma

MDSC Myeloid-Derived Suppressor Cell

MET Mesenchymal-to-Epithelial Transition

MMP Matrix Metalloproteinase

MAD Mitotic Arrest Deficient

MPS Monopolar Spindle

NLS Nuclear Localization Signal

NSCLC Non-small Cell Lung Cancer

PDGFR Platelet-Derived Growth Factor Receptor

PD-1 Programmed Cell Death Protein 1

PD-L1 Programmed Death Ligand 1

PDX Patient-derived xenograft

P/S Penicillin/ Streptomycin

PFA Paraformaldehyde

Poly-HEMA Poly 2-Hydroxyethyl Methacrylate

PRC Polycomb Repressive Complex

PRP4K Pre-mRNA Splicing Factor 4 Kinase

RA Retinoic Acid

RAL Retinal

RAR Retinoic Acid Receptor

RARE Retinoic Acid Response Element

RS Arginine-Serine Rich

RXR Retinoid X Receptor

RT-qPCR Reverse Transcriptase Quantitative Polymerase Chain Reaction

SAC Spindle Assembly Checkpoint

shRNA Short Hairpin Ribonucleic Acid

snRNP Small Nuclear Ribonuclear Particle

SP Side Population

SRSF Serine-Arginine Splicing Factor

STAT Signal Transducer and Activator of Transcription

TBST Tris Buffered Saline- Tween-20

TGF Transforming Growth Factor

TIC Tumor Initiating Cell

Acknowledgements

I wish to acknowledge everyone who has contributed to the progression and development of this project. A special thanks goes out to Dr. Graham Dellaire, my supervisor, for providing the support and input necessary to make this project what it is. I would also like to thank all of the members of the Dellaire Lab for their support. Furthermore, a big thanks to my committee members, Dr. Jeanette Boudreau and Dr. Jim Fawcett for their help in shaping the project, as well as the significant financial contributions provided by my co-supervisor Dr. Karen Bedard. Finally, I would like to thank my family and friends for their never-ending support, without whom this project would have never been possible.

Chapter 1: Introduction

1.1 Cancer

Cancer is most simply defined by uncontrolled cell proliferation and is a blanket term encompassing more than 275 cancer diseases¹. The first reported case of cancer occurred nearly 3000 years ago, and has since become the second leading cause of death worldwide, killing nearly 1 in 4 people^{2,3}.

The conversion of normal cells to cancer cells is extremely complex and involves the acquisition of so-called “Hallmarks of Cancer”. Originally published in 2001, the authors suggested six alterations that are essential for malignancy⁴. For example, cancer cells are able to proliferate even in the absence of exogenous growth stimulation, be it by cell-to-cell interaction or increased contact with diffusible growth factors. This can be accomplished through mutations in genes that allow these signals to remain active even in the absence of ligand and represents the first hallmark of cancer: self-sufficiency in growth signals. The increase in pro-survival signaling means that cancers also have a second hallmark: insensitivity to antigrowth signals. The sustained activation of pro-survival signaling pathways by growth factors also makes the cancer cells much less sensitive to the various forms of programmed cell death, leading to the third hallmark of cancer: evading apoptosis. Apoptosis can be the result of several different stressors, including the shortening of telomeres to the point where the cells are no longer able to survive. The fourth hallmark of cancer is limitless replicative potential and involves the upregulation of telomerase, an enzyme important in the lengthening of telomeres⁵. The final two hallmarks concern the behavior of the tumor *in vivo* and revolve around the ability of the tumor to metastasize (i.e. hallmark number five: tissue invasion and

metastasis) as well as its ability to modify its hosts' blood vessels to supply it with the oxygen required to sustain the growth of a rapidly dividing mass of cells (i.e. hallmark number six: sustained angiogenesis). Cancer cells are able to modulate the host blood supply through the use of secreted molecules that bind to host receptors⁶. The ability of cancer cells to metastasize is complex and involves a transition from an epithelial phenotype to a mesenchymal phenotype (epithelial-to-mesenchymal transition; EMT) as well as the ability to resist a form of detachment-induced apoptosis known as anoikis⁷. As mentioned, many of these hallmarks of cancer involve mutations (either activating or inhibitory) within key regulatory genes involved in these pathways; however, cells have mechanisms in place to detect and fix these mutations before the cell is able to progress to malignancy. The so-called "Guardian of the Genome" is a tumor suppressor known as p53, and it is no coincidence that the expression of p53 is lost in ~50% of all cancers⁸. Without this protein, cells are no longer able to efficiently correct mutations and therefore develop the enabling characteristic: genome instability, meaning they develop mutations more quickly and progress to malignancy more quickly.

In 2011, these same authors (Hanahan et al.) published a follow-up paper, wherein they amended the hallmarks of cancer and added four more, including the aforementioned genome instability⁹. One of these new hallmarks notes that cancer cells are able to regulate the way they produce their energy. The mechanism surrounding this is rather counterintuitive and involves the preferential use of glycolysis over oxidative phosphorylation (resulting in ~18 fold less ATP). This process is known as the Warburg effect and is hypothesized to occur to allow cancer cells to use glycolytic intermediates

for other purposes, such as generating nucleosides and amino acids, both of which are molecules crucial for sustaining rapid cell division^{10,11}.

The final additions also recognize the importance of anti-tumor immunity. When a normal cell becomes cancerous, it can begin to express certain proteins that the immune cells in the body are able to recognize as foreign either to the host (through mutations) or to that specific cell type (e.g. through expression of a normally embryonic gene in an adult)¹². Therefore, cancer cells need to find ways of avoiding immune destruction, be it through direct inhibition of the immune system (by upregulating surface proteins like PD-L1) or by “hiding” from the immune system (by inhibiting antigen presentation)^{13,14}. The final addition is tumor promoting inflammation, wherein recognition of a cancerous cell triggers inflammation, which can paradoxically promote tumor growth by triggering EMT, or facilitating angiogenesis^{15,16}. Taken together, cancer is a complex set of diseases and much more work is needed for us to fully understand its biology.

1.2 Lung Cancer

1.2.1 Introduction

Lung cancer remains the most common cause of cancer-related deaths worldwide, accounting for more than 1.6 million deaths per year¹⁷. Lung cancer is a molecularly heterogeneous disease and understanding its biology is critical for the development of targeted therapies. Lung cancers are typically divided up into two major types: small-cell and non-small cell, the latter accounting for ~85% of cases (Figure 1.1). Non-small cell lung cancer can then be further divided into four subtypes with the squamous cell carcinoma (LUSC) and adenocarcinoma (LUAD) subtypes being most prevalent¹⁸.

Between these two subtypes, adenocarcinomas are most common (making up ~35% of all lung cancers). The most common etiology of lung cancer is, perhaps unsurprisingly, tobacco smoke, which is responsible for ~80% of cases. While tobacco smoke has been shown to be associated with both major subtypes of lung cancer, adenocarcinomas are the most common among non-smokers¹⁹. LUAD can be further divided based on the driver mutation present in the tumor, which can, in turn, allow for targeted therapies. Common driver mutations include activating mutations in the epidermal growth factor receptor (*EGFR*) and *KRAS*, as well as inactivating mutations in *TP53*, *KEAP1*, and *NFI*^{20,21}. It is also important to note that the vast majority of LUAD tumors contain either *EGFR* or *KRAS* mutations, but almost never both, and those tumors that do contain both are far less sensitive to EGFR inhibitors versus having either one alone²². LUSC tumors, on the other hand, are characterized by *TP53* mutations (occurring in >90% of tumors) and mutations in *CDKN2A* (more commonly known as p16)²³. Because of this, LUSC tumors are much less, if at all, responsive to growth factor receptor inhibition²⁴.

1.2.2 Immunology

Immunologically, tumors can generally be divided into two types: those that are hot (i.e. have large numbers of infiltrated t-cells) and those that are cold (i.e. little to no immune infiltration and a highly immunosuppressive environment)²⁵. Non-small cell lung cancers (NSCLCs) are considered immunologically “warm” due to the presence of numerous types of immune cells with the presence of inhibitory molecules²⁶. For example, in NSCLC, approximately 50% of CD45+ immune cells are from the myeloid lineage with ~20% being neutrophils, while MDSCs comprise another ~10%, however, the role of

myeloid-derived suppressor cells (MDSCs) in lung cancer remains to be defined. While these tumors tend to have increased numbers of T-cells versus distal lung, it appears as those these T-cells are dysfunctional (i.e. express the immunosuppressive receptor PD-1 and show reduced IFN- γ production)^{27,28}. It should also be noted that within NSCLC tumors, macrophages as well as neutrophils had higher expression of PD-L1 (the PD-1 ligand) than did the tumor cells, thus contributing to an immunosuppressive environment²⁸.

On top of this, the approximate proportions of immune cell populations in human lung adenocarcinomas has only recently been examined by Stankovic et al. (2019), and it became clear that anywhere from 34-96% of all living cells in the bulk tumor are actually immune cells and of these, T-cells dominated (comprising ~47% of CD45⁺ cells), with CD19⁺ B-cells being the second most common (comprising ~16% of CD45⁺ cells). Considering most of these studies have only been published within the last two to three years, it appears that the intratumoral immune landscape of lung cancers in an emerging area and needs much more work to fully decipher.

1.2.3 Therapies

In terms of therapies, platinum-based dual therapies (e.g. cisplatin combined with another cytotoxic agent) have traditionally been the standard of care; however, over the last couple of decades, therapies are evolving to become more personalized depending on the molecular subtype (i.e. the driver mutation)²⁹. Despite this, surgery remains the most promising option for stage I and II lung cancers, and even then, a high proportion of tumors will recur, with a 5-year survival of 83% for stage I and 36% for stage III^{30,31}. It

has therefore been suggested that platinum-based chemotherapies be used in conjunction with surgical resection to maximize overall survival in early-stage diagnoses³². For the majority of patients, however, the cancer has already metastasized³³. For these patients, targeted therapies in conjunction with cytotoxic agents is standard. There are currently a number of targeted therapies for tumors harbouring activating *EGFR* mutations, with osimertinib currently being used as a first-line EGFR inhibitor³⁴.

A recent paper published in Nature showed the first evidence supporting the potential of a KRAS^{G12C}-specific inhibitor. This is important as ~13% of LUAD patients harbor a KRAS^{G12C} driver mutation. In this paper, the authors showed that the compound (AMG 510) was able to cause tumor regression in immunocompromised patient-derived xenograft (PDX) mouse models, but complete cures in immunocompetent mice suggested the requirement of an immune system. In humans, approximately half of the patients showed objective response to the drug. The authors also show that AMG 510 synergizes with immunotherapies and resulted in a nine times higher survival rate after five months compared to either AMG510 or anti-PD-1 therapy alone (in immunocompetent mice). The reason AMG 510 is more cytotoxic in the presence of an immune system is due to its ability to recruit immune cells (e.g. T-cells, macrophages, and dendritic cells) to the tumor. When mice cured of LUAD by AMG 510 were challenged with a KRAS^{G12D}-driven lung cancer, no tumor growth was detected, suggesting AMG 510 is resulting in the formation of an immune memory response to multiple forms of oncogenic KRAS mutations. This combined with the promotion of a pro-inflammatory environment (e.g. increased interferon production and antigen presentation) demonstrate the potential of this drug for the treatment of KRAS^{G12C}-driven tumors³⁵.

As previously mentioned, NSCLC tumors tend to have higher levels of PD-1 and PD-L1. This means that the use of checkpoint inhibitors (i.e. antibodies that block the interaction of PD-1 and PD-L1) should prove beneficial, and as it turns out, immune checkpoint inhibitors have recently been approved as the second line standard of care among patients who relapse or show tumor progression after treatment with platinum-based agents^{36,37}. On top of this, pembrolizumab is now the first-line treatment for patients having tumors with >50% PD-L1+ cancer cells (which occurs in ~30% of NSCLC patients)^{38,39}.

As opposed to other cancers, such as breast which have very clear subtypes, and treatments associated with most subtypes, lung cancer subtypes remain blurry and are still being established. Because of this, the best that can be done right now is surgery, and targeted therapies based on the tumor biology and profile of invading immune cells. Despite the presence of targeted therapies, lung cancer still has a 5-year survival of only 15%, and even after treatment, most people will relapse within 18-24 months, at which point the tumors will have metastasized, making them exponentially harder to treat⁴⁰⁻⁴². Because of this, we first need to be able to understand the underlying biology of these tumors if we hope to ever come up with effective treatments for them. One possible reason for the increased relapse rate of these tumors is the presence of a sub-population of tumor cells, known as cancer stem cells, which are highly radio- and chemoresistant, and are further described below⁴³.

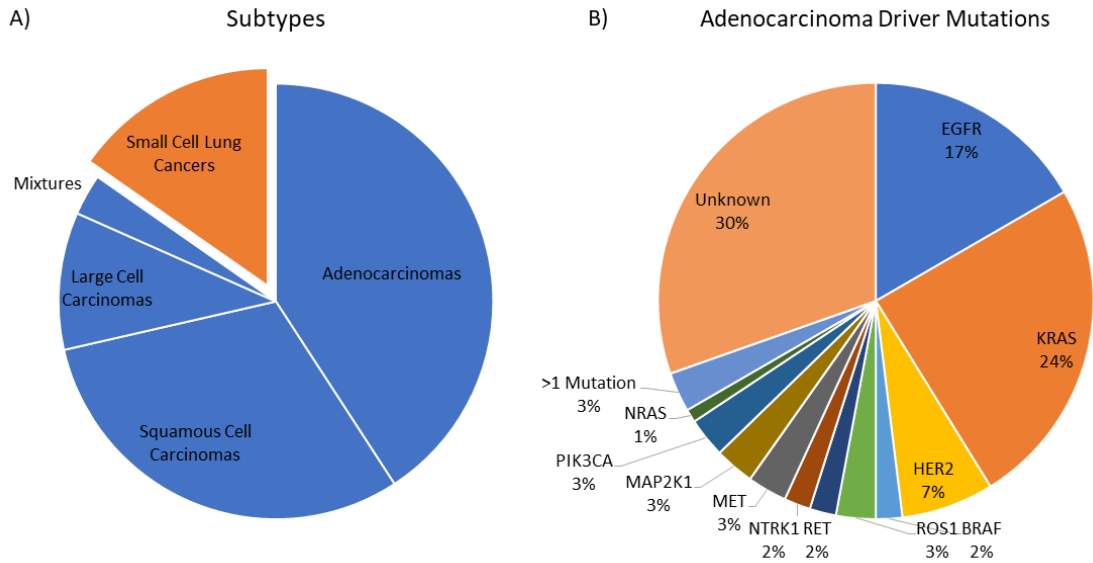


Figure 1.1. Lung cancer classification by histology and driver mutation breakdown. (A) Lung cancers are broken down into two major categories, with most being diagnosed as non-small cell lung cancers (blue) as opposed to small cell lung cancers (orange). Non-small cell lung cancers can be further broken down into subtypes with adenocarcinomas predominating. (B) breakdown of driver mutations common in adenocarcinomas with the majority of tumors having an unknown driver mutation.

1.3 Cancer Stem Cells

1.3.1 Introduction

Malignant tumors are not homogeneous masses of cells; in fact, within the last few decades, it has become clear that tumors consist not only of “normal” cancer cells, but they are also composed of a highly aggressive population of cells known as cancer stem cells (CSCs) or tumor initiating cells (TICs). CSCs were first characterized in 1997 by Bonnet and Dick, who isolated them from human acute myeloid leukemia patients. These cells were identified as being CD34⁺/CD38⁻ and were shown to be able to recapitulate the original tumor⁴⁴. Since then, CSC populations have been identified in a number of different cancers, including melanoma, breast, colon, prostate, pancreatic, brain, and lung⁴⁵⁻⁵¹. Although all these different cancers have CSCs, the markers used to identify them is cancer dependent. In all cases, however, CSCs have the unique abilities of self-renewal, tumor initiation, and the ability to reform tumors (consisting of both CSCs and differentiated non-CSCs)⁵².

In addition to these abilities, CSCs are highly chemo- and radioresistant, due in part to increased expression of efflux pumps (e.g. ABC transporters) as well as an enhanced ability to repair DNA damage⁵³⁻⁵⁵. Since CSCs are resistant to most first-line treatments, conventional therapies are most effective in removing “normal” cancer cells; however, since they leave CSCs behind, the cancer is allowed to recur and metastasize, contributing to ~90% of cancer-related deaths^{56,57}.

1.3.2 Identification

CSCs are most commonly identified through the use of flow cytometry, allowing for single-cell resolution of protein markers which can help identify these cells from non-CSCs or normal stem cells⁵⁸. Commercial kits are also available for identifying CSCs using the ALDEFluor reagent (a reagent that becomes fluorescent after interacting with aldehyde dehydrogenases; ALDHs). *In vivo* assessments of CSC frequency can be performed using a technique called a limiting dilution assay, whereby different numbers of cells are injected into animals and tumor formation frequency is recorded⁵⁹. This allows researchers to calculate the frequency of CSCs since, for example, a population with a high proportion of CSCs would require less cells to form a tumor.

1.3.3 Origins

Currently, there are two schools of thought regarding the development of CSCs. One side of the debate supports the original theory, derived from studies in leukemia, whereby CSCs arise from normal stem cells that have acquired mutations to become malignant⁶⁰. The other side, which is more accepted, states that normal tissue cells develop mutations which cause them to become cancerous. As time goes on, these cancer cells will develop mutations in genes which allow them to “de-differentiate”, giving them properties of both stem cells *and* cancer cells⁶¹.

1.3.4 Relationship with Epithelial-to-Mesenchymal Transition

Another potential mechanism for the development of CSCs is for cancer cells to undergo EMT, or the reverse process MET, and develop into a stem-like phenotype. This is

evidenced in lung cancer cell lines where CD44^{high}/ALDH⁺ cells have significantly increased expression of mesenchymal markers vimentin, Zeb1, and Slug, along with increased expression of the stemness-associated Yamanaka factors Sox2, Oct4, and Nanog, and a decrease in the expression of the epithelial marker E-cadherin when compared to CD44^{low}/ALDH⁻ cells⁶². This also suggests the existence of a “stemness window”, a hybrid-EMT state in which cells show increased tumor initiation capabilities, collective migration and have weak cell-cell connections⁶³.

EMT, as previously mentioned, is not a simple one step process, but is rather a spectrum of phenotypes ranging from fully epithelial to fully mesenchymal with intermediate phenotypes in between. These intermediate phenotypes may not necessarily just be a midpoint in the conversion of one to the other but may in fact be the cell’s final fate⁶⁴. These so-called “partial (or hybrid) EMT states” are often found to be a marker of worse prognosis in cancer patients due to their increased plasticity and increased metastatic potential⁶⁵. There are a number of different methods used to identify hybrid EMT states, one of which is by using the following groups: epithelial (E-Cadherin [CDH1] positive, cytokeratin positive, vimentin negative), intermediate epithelial (E-cad⁺ CK/Vim^{+/+}), intermediate mesenchymal (E-cad⁻ CK/Vim^{+/+}), and mesenchymal (E-cad⁻ CK/Vim^{-/+})⁶⁶. These authors also determined that only about half of patient cells in a partial EMT state are characterized as expressing another mesenchymal marker, CDH2 (N-Cadherin) and that cells in the intermediate mesenchymal state have the highest sphere-forming ability (i.e. most stem-like) of all EMT states. This stem-like phenotype has also been shown by another group studying breast cancer, who found that cells in a completely mesenchymal state form mammospheres less efficiently than those in

intermediate states⁶⁷. Few groups have attempted to characterize these intermediate phenotypes in the context of lung cancer, however one group showed that lung cancer cells in a partial EMT state express both CDH1 and the EMT transcription factor SNAI2 (Slug)⁶⁸. To summarize, there is no question that partial EMT states exist, however the identification and characterization of these phenotypes is still under investigation.

One of the more important outcomes of being in an intermediate EMT state is that cells are able to maintain cell-to-cell contact while also surviving growth in non-adherent conditions (i.e. detached from the basement membrane). This allows clusters of cells to migrate through the bloodstream to other areas of the body and allows for an ~50-fold increase in metastatic success versus single cells alone⁶³. The relationship between EMT and stemness is summarized below in Figure 1.2

As mentioned, the key roles of CSCs are highly conserved⁶⁹. One explanation for this is that there are regulatory pathways that are commonly dysregulated within this population of cells, regardless of the type of cancer. Examples of these pathways include Wnt, Notch, Hedgehog, as well as janus kinase/ signal transducer and activator of transcription (JAK/ STAT) and the stemness-associated transcription factors Sox2, Oct4, and Nanog (together, the last three are known as the Yamanaka factors)⁷⁰⁻⁷⁵.

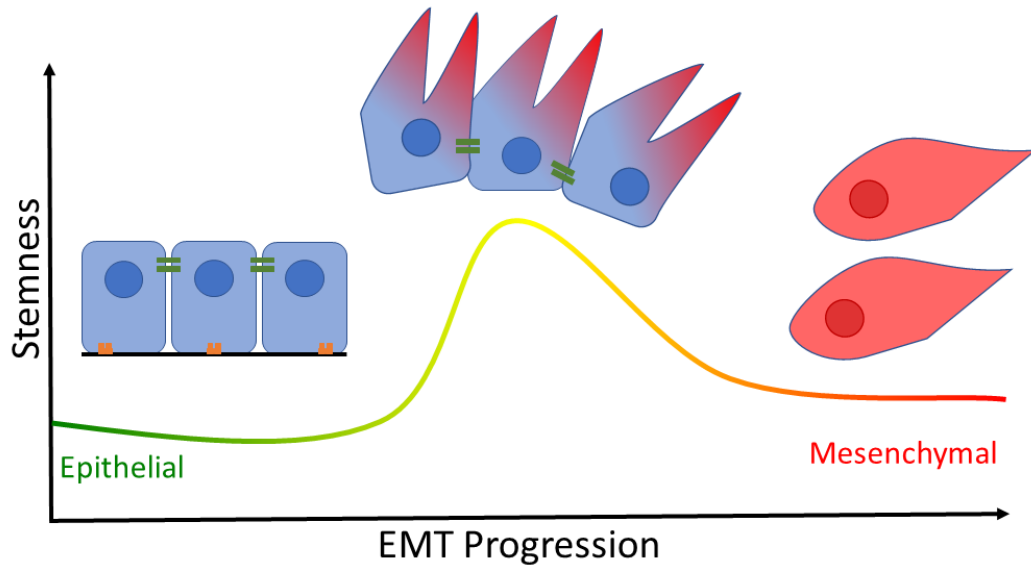


Figure 1.2 Relationship between stemness and EMT progression. As cells progress through EMT, they reach a point of peak stemness/ malignancy, when they possess characteristics of both epithelial and mesenchymal cells, such as the ability to maintain cell-cell contact, resist anoikis, and gain the ability of self-renewal. Adapted from Malfettone et al. (2017)⁷⁶.

1.4 Lung Cancer Stem Cells

1.4.1 Introduction

Unlike other types of CSCs, such as those found in breast cancer, lung CSCs (LCSCs) seem to be much more diverse and their identification by flow cytometry is still under investigation. The most common and agreed upon ways to identify LCSCs would be as side population (SP) positive (i.e. high expression of ATP-dependent efflux pumps), ALDH⁺, CD44⁺, and/or CD133⁺ cells⁷⁷⁻⁸⁰. For the sake of this project, expression of CD44 as well as ALDH activity were the two primary methods used for identification since they are the most common markers not only for lung, but also other cancer types, such as breast, glioblastoma, colorectal, and gastric⁸¹⁻⁸⁴.

1.4.2 Aldehyde Dehydrogenases

The ALDH superfamily has 19 different isoforms with distinct functions and specificities⁸⁵. ALDH enzymes can be broadly divided into two categories 1) those that are highly substrate specific and necessary for normal development and 2) those that are less substrate specific and primarily detoxifying⁸⁶. Therefore, there is a large degree of diversity among the ALDH enzymes, leading to an important question; which ALDH isoform contributes to the ALDEFfluor^{hi} activity observed among LCSCs?

In 2014, ALDH1A3 was shown to be the major contributor to ALDH activity in NSCLC CSCs, wherein ALDH⁺ cells were enriched in ALDH1A3, tumorigenicity, and clonogenicity. Furthermore, it was also found that in these cells, ALDH1A3 mediates CSC properties through STAT3 signaling, which can further increase expression of ALDH1A3, indicating the existence of a positive feedback loop between the activity of

the two proteins⁷⁹. This also provides potential therapeutic targets for these patients. It has also been shown that ALDHs are involved in the production of retinoic acid (RA) via the oxidation of retinal (RAL) by ALDH1A3⁸⁷. RA then binds to retinoic acid receptors (RARs) and retinoid X receptors (RXRs); both of which are nuclear hormone receptors. RARs and RXRs exist primarily as heterodimers that are bound to specific parts of the DNA called retinoic acid response elements (RAREs). Without RA, the nuclear co-repressor protein prevents transcription by recruiting repressive factors such as histone deacetylase complexes (HDACs) and the polycomb repressive complex 2 (PRC2). In the presence of RA, a conformational change results in co-repressor release and co-activator recruitment causing the transcription of genes regulated by RAREs^{88,89}. It is currently accepted that RA signaling induces differentiation in stem cells and may thus provide an avenue for treating cancers by depleting tumors of CSCs^{90,91}.

There is also evidence that, when used together, CD44 and ALDH activity can be used to isolate multiple sub-populations of LCSCs with varying degrees of tumorigenicity. For example, in adenocarcinoma LCSCs, tumorigenicity and chemoresistance is more heavily reliant on ALDH activity than CD44 surface expression, creating a spectrum of tumorigenicity in which CD44⁺/ALDH⁺ and CD44⁻/ALDH⁺ LCSCs form tumors that are larger and form quicker than CD44⁺/ALDH⁻ or CD44⁻/ALDH⁻ cells⁶². In addition to the ALDH⁺ phenotype, LCSCs can be identified by CD44 surface staining.

1.4.3 CD44

CD44 is a transmembrane glycoprotein that interacts with extracellular matrix ligands such as hyaluronic acid, matrix metalloproteinases (MMPs), collagenases and

osteopontin⁹²⁻⁹⁵. This mediates many important CSC-related characteristics such as cell survival, migration, invasion, angiogenesis, and metastasis⁹⁶. CD44 has multiple isoforms due to the insertion of alternative exons in the region of the transcript coding for the extracellular domain. The main isoform in LCSCs depends on the cell line under investigation. For example, the major CD44 isoform in Lewis Lung carcinoma (LLC) cells is CD44s which activates the platelet-derived growth factor receptor 3 (PDGFR β) and STAT3 cascade to promote CSC traits^{97,98}. The different isoforms are denoted as CD44s, representing the fully spliced form and CD44v which represents some form of exon inclusion.

1.4.4 Hyaluronic Acid

Another important component of CD44 signaling is the role of the CD44 ligand: hyaluronan (also known as hyaluronic acid; HA). The biosynthesis of hyaluronic acid was first described in 1969 in *Streptococcus spp*⁹⁹. Since then, it has become clear that hyaluronic acid exists in two major forms with differing functions: high molecular weight (HMW-HA) and low molecular weight (LMW-HA)¹⁰⁰. HMW-HA promotes an anti-tumor environment by inhibiting proliferation of cancer cells, slowing their migration/ invasion, and protecting cells from DNA damage caused by reactive oxygen species¹⁰¹⁻¹⁰⁴. LMW-HA, on the other hand, has the opposite effect, it promotes neo-angiogenesis, cancer cell proliferation, and migration/ invasion¹⁰⁵. The HA biosynthetic pathway involves a class of enzymes known as hyaluronan synthases (HAS) 1-3. Each of these isoforms localizes to a different compartment, with HAS2 being primarily found at the plasma membrane¹⁰⁶. From here, HAS2 uses alternating units of UDP-D-Glucuronic acid

and UDP-N-Acetyl-Glucosamine to form HMW-HA which is released directly into the extracellular space as it is being synthesized. After that, the HMW-HA is cleaved by hyaluronidases (HYALs) to form LMW-HA which is able to activate the CD44 signaling cascade within the same cell the HA was originally produced, mimicking a form of “autocrine” signaling in these cancer stem cells. This also speaks to the potential clinical benefits of inhibiting HA synthesis in cancer patients whose tumors have high HAS and/or HYAL expression¹⁰⁷. The small molecule 4-Methylumbelliferone (4-MU) is used to inhibit HA synthesis *in vitro* and does so potentially by both decreasing mRNA levels of HAS2 and HAS3 but also by mimicking UDP and inhibiting the actual HA biosynthesis by HAS and downregulating CD44 expression^{108,109}. While there are currently no known clinical trials using 4-MU for the treatment of cancer, research has suggested it is well tolerated in humans at doses up to 2400 mg/kg for up to three months and is currently being used to treat bile duct disorders¹¹⁰. Recent evidence *in vitro* using a number of different cancer types has suggested its efficacy in inhibiting tumorsphere formation^{111,112}.

1.5 Pre-mRNA Splicing Factor 4 Kinase (PRP4K)

PRP4K is an ~150 kDa protein composed of 1007 amino acids and contains the splicing associated KKHK and RS domains. It is a dual-specificity kinase and contains two highly conserved motifs involved in substrate recognition: MI (DDMFA) and MII (DNWTDAEGYYRV)¹¹³. See Figure 1.3 below for the structure of mouse PRP4K.

PRP4K localizes to the nucleus but is excluded from the nucleolus and plays a role in assembling the spliceosome¹¹⁴. Two of the major PRP4K substrates are the pre-

mRNA processing factor proteins PRP6 and PRP31, which are required to join the tri-small nuclear ribonucleoprotein (tri-snRNP) to complex B^{113,114}. In addition, PRP4K has been shown to co-purify with the U5 snRNP and phosphorylates the serine arginine splicing factor SRSF1, a protein essential for 5' splice site selection and alternative splicing^{113,114}. Taken together, these studies suggest an important role for PRP4K in alternative splicing.

PRP4K has also been found to have a role as a potential spindle assembly checkpoint (SAC) protein. One paper found that low PRP4K prevents the recruitment of known SAC proteins, such as monopolar spindle 1 (MPS1), mitotic arrest deficient protein 1 (MAD1), and mitotic arrest deficient protein 2 (MAD2). This causes chromosomal mis-segregation and results in resistance to the microtubule depolymerizing agent nocodazole¹¹⁵.

Due to its role as a SAC protein, the Dellaire lab was interested as to how cancers with low levels of PRP4K respond to the microtubule-stabilizing chemotherapy paclitaxel. They found that when breast and ovarian cancers have low levels of PRP4K, cells fail to undergo mitotic arrest in the presence of paclitaxel, and instead re-enter the cell cycle without dividing. In the same paper, the authors showed that treating cells with 4-Hydroxytamoxifen (4-OHT; an estrogen receptor antagonist) resulted in lower levels of PRP4K, suggesting the potential of PRP4K as a biomarker for chemotherapy response¹¹⁶. In a subsequent paper, Corkery et al. found that knockdown of PRP4K resulted in increased metastasis in the ID8 model of ovarian cancer and increased expression of EMT markers vimentin and TrkB¹¹⁷. In this same paper, authors also showed that

knocking down PRP4K in these cell lines resulted in anoikis resistance, providing further support for the role of PRP4K in EMT.



Figure 1.3 Protein Structure of PRP4K. Protein Structure of mouse PRP4K. Adapted from Dellaire et al. (2002)¹¹³.

1.6 Rationale/ Hypothesis

As the role of PRP4K in lung cancer has yet to be investigated, I sought to determine what role, if any, it was playing in this context. Preliminary data suggested that lowering the levels of PRP4K resulted in significantly shorter time to tumor development as well as increased growth rates, leading to the hypothesis that PRP4K play a role in inhibiting the acquisition of “stemness” in lung cancer cells. In this study, I hope to determine the mechanism by which low PRP4K can regulate stemness using a murine model of lung cancer, the Lewis Lung Carcinoma cell line, which is syngeneic to C57BL/6 mice.

Chapter 2: Methods

2.1 Cell lines and Cell Culture

LLC cells were purchased from ATCC Cell Lines and were cultured in DMEM supplemented with 5% FBS and 1% P/S.

2.2 Generation of PRP4K Lentiviral Knockdowns

Stable PRP4K short hairpin ribonucleic acid (shRNA) knockdown clones were generated using two separate targeting shRNAs and two non-targeting shRNAs. Lentiviral particles were generated using lentiviral vector SMARTvector with either the shRNA scramble sequences or shRNA sequences specific to PRP4K. shRNA binding sites on the mouse PRP4K transcript are shown in Figure 2.1. HEK293T cells were transfected using calcium phosphate along with packaging plasmids (5 ug psPAX2, 5 ug pMDG.2, 10 ug of control or shPRP4K specific sequences). Sixteen hours after transfection, 293T media was replaced with DMEM containing 0.1% FBS. Two days later, the 293T cell supernatants containing lentivirus were collected, filtered through a 0.45 um filter, and applied to cultured LLC cells and selection of stable transfectants began 4 days post transduction with the addition of 2 µg/mL puromycin (Sigma Aldrich). Clones were maintained in their respective culture media containing 2 µg/mL puromycin. Knockdown was confirmed using RT-qPCR, immunofluorescence, and Western Blotting (See Methods sections 2.3, 2.4, and 2.6). Plasmids used in this study are shown in Table 1.

Table 1. Plasmids used in this study

| Plasmid | Clone ID | Source |
|-----------------------|------------------|-----------|
| psPAX2 | 12260 | Addgene |
| pMD2.G | 12259 | Addgene |
| SMARTvector Control 1 | VSC11279 | Dharmacon |
| SMARTvector Control 2 | VSC11722 | Dharmacon |
| SMARTvector shPRP4K-1 | V3SVMMC_17028226 | Dharmacon |
| SMARTvector shPRP4K-2 | V3SVMMC_12040771 | Dharmacon |



Figure 2.1 Location of processed shRNA binding on the mouse PRP4K transcript beginning with exon one (left) and ending with exon 15 (right). Clone 1 binds the transcript at bases 1375-1388 and Clone 2 binds bases 809-816.

2.3 Western Blots

Cells were harvested using a cell scraper, placed in 1.5 mL microcentrifuge tubes, and stored at -80°C for further analysis. Pellets were resuspended in and lysed using ice-cold lysis buffer (20mM Tris-HCl pH8, 300mM KCl, 10% Glycerol, 0.25% Nonidet P-40, 0.5mM EDTA, 0.5mM EGTA, 1x protease inhibitors) prior to mechanical DNA disruption through the use of 22-gauge needles. Lysates were then cleared by centrifugation (25min, 15 000xg, 4°C) prior to polyacrylamide gel electrophoresis run at 50 V for 30 minutes and then 120 V for two hours. Proteins were then transferred to nitrocellulose at 100 V for one hour. Blots were then stained with ponceau to ensure proper transfer prior to a 45-minute block in 5% w/v milk powder in TBST. Primary antibody staining (1:1000-1:10000) was carried out overnight at 4°C proceeded by a one-hour incubation with an HRP-conjugated secondary antibody (1:5000). Blots were analyzed using ECL and images taken using a Chemidock (BioRad) or film. Antibodies used in this study are shown in Table 2 and full-length blots are located in Appendix 2.

Table 2 Primary and secondary antibodies used in this study. WB: Western Blot, IF: Immunofluorescence, FC: Flow Cytometry.

| Primary | Fluorochrome | Secondary | Assay | Company (Product Number) | Dilution |
|-------------|--------------|--------------------------------------|--------|--|----------|
| Tubulin | N/A | G α M HRP | WB | Santa Cruz Biotechnology (sc-9104) | 1:10000 |
| ALDH1A3 | N/A | G α Rb HRP | WB | Abcam (ab129815) | 1:1000 |
| Fibronectin | N/A | G α Rb HRP | WB | Abcam (ab2413) | 1:1000 |
| Vimentin | N/A | G α Rb HRP | WB | Cell signaling (5741) | 1:1000 |
| Snail | N/A | G α Rb HRP | WB | Cell signaling (3879) | 1:1000 |
| Slug | N/A | G α Rb HRP | WB | Cell signaling (9585) | 1:1000 |
| E-Cadherin | N/A | G α Rb HRP | WB | Cell signaling (3195) | 1:10000 |
| Crabp1 | N/A | G α Rb HRP | WB | Cell signaling (13206) | 1:500 |
| PRP4K | N/A | G α Rb HRP, G α Rb 647 | WB, IF | Novus Biologicals (NBP1-82999) | 1:2500 |
| CD44 | PE, N/A | N/A, G α Rt HRP | FC, WB | Invitrogen (12-0441- 81 and 14-0441-82) | 1:1000 |

2.4 Immunofluorescence Microscopy

Cells were cultured in 6-well plates containing an 18mm x18mm Type 1 coverslip for 24 hours, at which point coverslips were rinsed in PBS prior to fixation in 2% PFA for 20 minutes. Coverslips were then rinsed and permeabilized using 0.5% Triton X-100 for 5 minutes. Cells were blocked in 5% donkey serum for 20 minutes and immediately placed into primary antibody (1:200; Table 2) diluted in 5% donkey serum for one hour at room temperature. Coverslips were then rinsed in PBS and incubated for 30 minutes in the dark at room temperature in fluorescently tagged secondary antibody. Excess antibody was rinsed off using PBS and nuclei were stained for ten minutes at room temperature using DAPI (Sigma-Aldrich, D9564) diluted at 1:1000. Coverslips were mounted on sterile slides, sealed using clear nail polish and stored at 4°C until analysis. Images were taken using a Zeiss LSM 710 confocal microscope under a 63× immersion oil objective lens. Images were then processed using only linear adjustments (e.g. brightness/contrast) with Slidebook (Intelligent Imaging Innovations, Boulder, CO) and Adobe Photoshop CC 2014.

2.5 ALDEFluor Assays

Approximately 1×10^6 cultured LLCs were washed once with PBS, trypsinized, and centrifuged at 500g for 3 minutes. Next, the cells were resuspended in Aldefluor Buffer containing the BODIPY® -aminoacetaldehyde (BAAA) substrate (as per manufacturer's instructions: Aldefluor Assay Kit [Stem Cell Technologies]). Cells were incubated at 37°C for 15 minutes. After the incubation period, cells were spun at 500 x g and then stained with 7-AAD (BioLegend) to a final dilution of 1:200. A control sample treated

with Aldefluor activity-inhibitor diethylaminobenzaldehyde (DEAB; as per manufacturer's instructions) was included for each sample to ensure that the ALDEFuor⁺ population of cells had been correctly gated. Side-scatter (SSC) and forward-scatter (FSC) gating was used to remove debris and doublets from analysis while 7-AAD was used to remove dead cells¹¹⁸. Data was collected using the FACSCanto II (BD BioSciences), and then processed using FCSExpress 5 RE Software.

2.6 Flow Cytometry

To assess the effect of PRP4K knockdown on the CD44⁺ populations, cells were collected, washed in PBS and then resuspended in FACS buffer (PBS supplemented with 5% FBS) containing a CD44 (0.5 uL/mL) monoclonal antibody (eBioscience). Cells were incubated at room temperature for 30 minutes. Following incubation, cells were resuspended in FACS buffer containing viability dye 7-AAD (5uL/mL). In cases where CD44 staining was paired with ALDEFuor activity, staining was done after incubation in BAAA and antibody staining was carried out in ALDEFuor Buffer. Flow cytometry was performed, and data collected using the FACSCanto II (BD BioSciences), and then processed using FCSExpress 5 RE Software. Gates were placed as dictated by single stain and unstained controls.

2.7 RT-qPCR

For sample collection, media was removed from cells and 500 uL TRIZOL was added to each well of a 6-well plate (Corning). RNA was extracted using the PureLink RNA MiniKit (Life Technologies) as per the manufacturer's guidelines. Exceptions include the

use of 125 μ L of chloroform and a larger elution volume (50 μ L). RNA was quantified by measuring absorbance at 260nm and 280 nm with NanoDrop 2000 Spectrophotometer. Complementary DNA (cDNA) was made by reverse transcribing 1 μ g of RNA using iScript RT Supermix (BioRad) as per manufacturer's guidelines. Individual samples were assayed in triplicate using a 96-well plate (BioRad) or 384-well plate (BioRad) and BioRad CFX Connect™ or BioRad 384™ qPCR machine. Each reaction consisted of 1 μ L cDNA, 5 μ L 2X SsoAdvanced™ SYBR® Green Supermix, 0.5 μ L of 10 μ M forward primer, 0.5 μ L of 10 μ M reverse primer, and 3 μ L NF-H₂O for a 10 μ L total reaction. Plates were then centrifuged and reactions amplified using the following thermal profile: 30 seconds at 95°C, followed by 40 cycles of 5 seconds at 95°C and 15 seconds at 60°C. Melt curve analysis was also performed on all plates to ensure only one product was made by increasing the temperature from 65°C to 95°C in 0.5°C increments every five seconds. BioRad CFX Maestro (BioRad) Software was used to normalize data to reference genes. Reference gene stability was also assessed using geNorm expression stability value of the reference gene (M) and the coefficient of variation of the normalized reference gene relative quantities (CV). The default limits for these values are 1 and 0.5 for M and CV, respectively¹¹⁹. Primer sequences were designed using NCBI Primer Blast (Table 3) and MIQE guidelines were followed throughout. Actin and Cytochrome C were used as reference genes.

Table 3 Primers used in this study. All primers were designed to be intron spanning and detect all transcript variants.

| Gene | Forward Primer | Reverse Primer |
|--------------|---------------------------|---------------------------|
| Actin | ACAGCAGTTGGTTGGAGCAAA | TTTTGGGAGGGTGAGGGACTT |
| Cytochrome C | ACACAGAAGTCTTGGAGTATGATGA | CAAGATGACAAGCAGATACTGAACA |
| PRP4K | GCTGAGGAGAAGATGAAGAGTGAA | TCCGCTCTTTGGACCTTGAC |
| CD44 | CGCTACGCAGGTGTATTCCA | TGCTCAGGGCCAACTTCATT |
| ALDH1A3 | CGGAGAGTGCGAACCAGTTA | TCCACTCTTGGATTCGTGCC |
| Fibronectin | GGTTCGGGAAGAGGTTGTGA | TGGCGTAATGGGAAACCGTG |
| E-Cadherin | GTCAGTTCAGACTCCAGCCC | AAATTCACTCTGCCCAGGACG |
| Snail | AGTTGACTACCGACCTTGCG | TGCAGCTCGCTATAGTTGGG |
| Vimentin | GGATCAGCTACCAACGACA | AAGGTCAAGACGTGCCAGAG |
| Crabp1 | CGTGGAGATCCGCCAAGAC | CCAAATGTCCTGCATTTGCGT |

2.8 Anoikis Assays

For anoikis assays, the LLC shRNA knockdown cells were seeded at approximately 50% confluence on Poly-HEMA coated 6-well plates. One day post-seeding cells were washed with PBS, collected and resuspended in annexin V binding buffer (0.1M HEPES (pH 7.4), 1.4M NaCl, and 25 mM CaCl₂; diluted 1/5 with dH₂O). The cells were then incubated with annexin V conjugated to FITC (Invitrogen Thermo Fisher Scientific) at room temperature for 15 minutes. Following the incubation, cells were pelleted and resuspended in annexin V binding buffer containing 7-AAD (5uL/mL). Flow cytometry was performed, and data collected using a FACSCanto II (BD BioSciences) and processed with FCS Express 5 RE software (De Novo Software).

2.9 Transwell Assays

Growth factor-containing medium (supplemented with 20% FBS) was added to the lower chamber and cells (1×10^4 for migration and 5×10^4 for invasion) reconstituted in serum-free medium were added to the upper chamber of 24-well plates. After 24 hours, the non-migratory cells on the inside of the insert were removed. Inserts were then washed with PBS and fixed with methanol for 15 minutes. Following fixation, inserts were washed with PBS and stained with 0.5% crystal violet for 30 minutes. Inserts were then washed until clear of excess stain. Images of the inserts were taken using an Olympus CKX41 microscope. The images were quantified using ZEN lite 2012.

2.10 Tumorsphere Assays

Cells were trypsinized and centrifuged at 500g for three minutes and pellets resuspended in serum-free DMEM/F12. Cells were then counted and diluted to 1.98×10^5 cells/ mL and plated at 5000, 1000, 500, or 100 cells per well in a Poly-HEMA-coated 12-well plate (Corning). Wells were then topped up to 1 mL per well with CSC media (DMEM/F12 supplemented with 10 ng/mL bFGF (Gibco), 20 ng/mL EGF, and 1x B27 [Gibco]). Cells were incubated at 37°C in 5% CO₂ for ~5-7 days prior to counting using an inverted microscope.

2.11 Proliferation Assays

Cells were plated at 50,000 cells per mL into 6-well plates with either DMSO, 50 nM RA, or 100 nM RA in media containing charcoal-stripped FBS. Every 24 hours, cells were trypsinized and counted using a Moxi Z Cell Counter (Orflo).

2.12 Animal Experiments

All experimental procedures were approved by the Dalhousie University Committee on Laboratory Animals following the guidelines of the Canadian Council on Animal Care. For clonogenic assay, 8-10-week-old female C57/BL6 mice (Charles River Laboratories) were injected subcutaneously with 5×10^5 LLC shCtrl or LLC shPRP4K cells. Tumor growth and survival were followed for 23 days post-injection at which point, tumors and spleens were dissociated into single cells suspensions and analyzed by flow cytometry. Lungs were removed with one being used for histologic analysis and the other being used

for clonogenic assay (described below in 2.13). Experimental designs are shown in Figure 2.2.

2.13 Clonogenic Assay

Lungs were aseptically removed from mice and a cell strainer was used to obtain a single-cell suspension in Hanks' Balanced Salt Solution supplemented with 10% FBS. Cells were then centrifuged at 300g for five minutes and the pellets were resuspended in sterile ammonium chloride for three minutes to lyse red blood cells. The reaction was terminated by adding complete DMEM prior to centrifugation and another rinse with complete media. Cells were then resuspended and plated in 6-well plates for ~10 days at which point media was removed and cells were fixed for five minutes in 100% methanol. Staining was carried out by incubation at room temperature in 0.5% crystal violet.

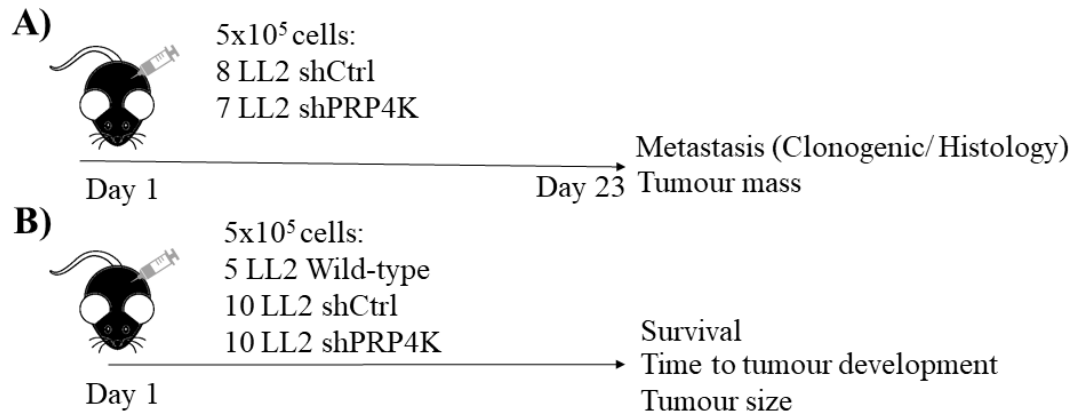


Figure 2.2 Experimental design for in vivo experiments. (A) Preliminary experiment used to determine tumor growth rates and metastasis. (B) Endpoint experiment used to determine survival and tumor size (included extra controls and knockdowns compared to initial experiment).

2.14 Statistics

All graphs were made using GraphPad Prism 6. For all graphs, tests for normality were performed to ensure the proper test was chosen. For conditions where two groups are being compared, a student's t-test was used (two-tailed). For experiments with three or more groups, a one-way ANOVA was carried out while experiments containing more than one independent variable used a two-way ANOVA. For all ANOVAs, Tukey's post-hoc analysis was used to determine significance between groups. Analysis of tumor growth *in vivo* was carried out linear regression to determine differences in slope between groups. Kaplan Meier survival was analyzed using a Log-rank (Mantel-Cox).

Chapter 3: Results

3.1 Depletion of PRP4K by shRNA Induces Features of Cancer Stem Cells in the Mouse Lewis Lung Carcinoma Model

The two most common types of lung cancer are squamous cell carcinoma and adenocarcinoma, however low PRP4K is only associated with worse overall survival among adenocarcinoma patients. Given that adenocarcinoma patients are comprised of both smokers *and* non-smokers, I wondered how this factored into patient survival. As it turns out, low PRP4K is associated with worse overall survival among both groups (Figure 3.1). Since the role of PRP4K had never been examined in lung cancer I chose to utilize the Lewis Lung Carcinoma model of murine non-small cell lung adenocarcinoma. I chose this cell line as it would allow me to take my experiments *in vivo* and was, to the best of my knowledge, the only syngeneic model of lung cancer that existed when these experiments began. To that end, I began by knocking down PRP4K and validating the knockdown in three different ways: RT-qPCR, Western Blot, and immunofluorescence microscopy across a total of six passages. All three of these methods showed comparable results, with shPRP4K-1 being approximately 90% knocked down and shPRP4K-2 being approximately 50% knocked down (Figure 3.2).

Given the high rates of recurrence in lung cancer, and previously published work on the relationship between PRP4K and anoikis/ EMT and chemoresistance, I first sought to determine whether knocking down PRP4K has an effect on cancer stem cells as these phenotypes are commonly associated with CSCs (See section 1.3 above)^{117,120}. To do this, I performed a limiting dilution assay *in vitro*, the results of which showed that knocking down PRP4K resulted in a significantly increased number of tumorspheres in

both shRNAs and the number of spheres formed was positively correlated with the degree of knockdown (Figure 3.3). This provided evidence that knockdown of PRP4K was increasing the number of CSCs within this population of cells.

To further elucidate the mechanism behind this, I examined some classical CSC markers by flow cytometry. I found that the shCtrl and shPRP4K-1 lines had ~40% ALDEfluor positive cells, while the shPRP4K-2 line had more, at ~70% ALDEfluor positive cells (Figure 3.4 A). As for CD44, I observed no change in surface expression between the shCtrl or shPRP4K lines (Figure 3.4 B). To follow up on this, I performed Western Blots for both CD44 (using an unlabeled version of the flow cytometry antibody), as well as ALDH1A3 (the primary contributor to ALDEFluor activity in LCSCs). I found that consistent with the flow cytometry, PRP4K knockdown increased protein levels of ALDH1A3 in both shRNAs by ~2-3-fold. Unlike the surface expression of CD44, however, I observed a decrease in total CD44 levels. This Western Blot also tells me that despite being primarily investigated for its role in splicing, knockdown of PRP4K does not seem to be causing a protein isoform switch in CD44. This is evidenced by similar banding patterns between the shCtrl and shPRP4Ks (Figure 3.5 A). I further determined that the CD44 transcript is decreasing proportionally to the protein levels, whereas the ALDH1A3 transcript levels are not changing, providing further insight into how PRP4K is regulating their expression (Figure 3.5).

Since HA has been shown to play a role in mediating CSCs, I next sought to determine if PRP4K knockdown was utilizing this pathway to cause its CSC effects. To that end, I first tested whether the PRP4K KD cells were more sensitive to the inhibition of HA synthesis using the small molecule 4-MU. I found that while both the shCtrl cells

and the shPRP4K cells responded to the compound, the shPRP4K cells responded to a higher degree, with the controls showing a 44% decrease in sphere number at 0.25 mM and the PRP4K shRNAs showing a 56% decrease (Figure 3.6 A). This indicated that HA synthesis was potentially involved, so I next wanted to try and mimic the CSC phenotype in the shCtrl cells by exposing them to exogenous HA. In this case, I found that both PRP4K shRNAs didn't show a significant response, while the shCtrl cells doubled the number of tumorspheres in the presence of exogenous HA (Figure 3.6 B).

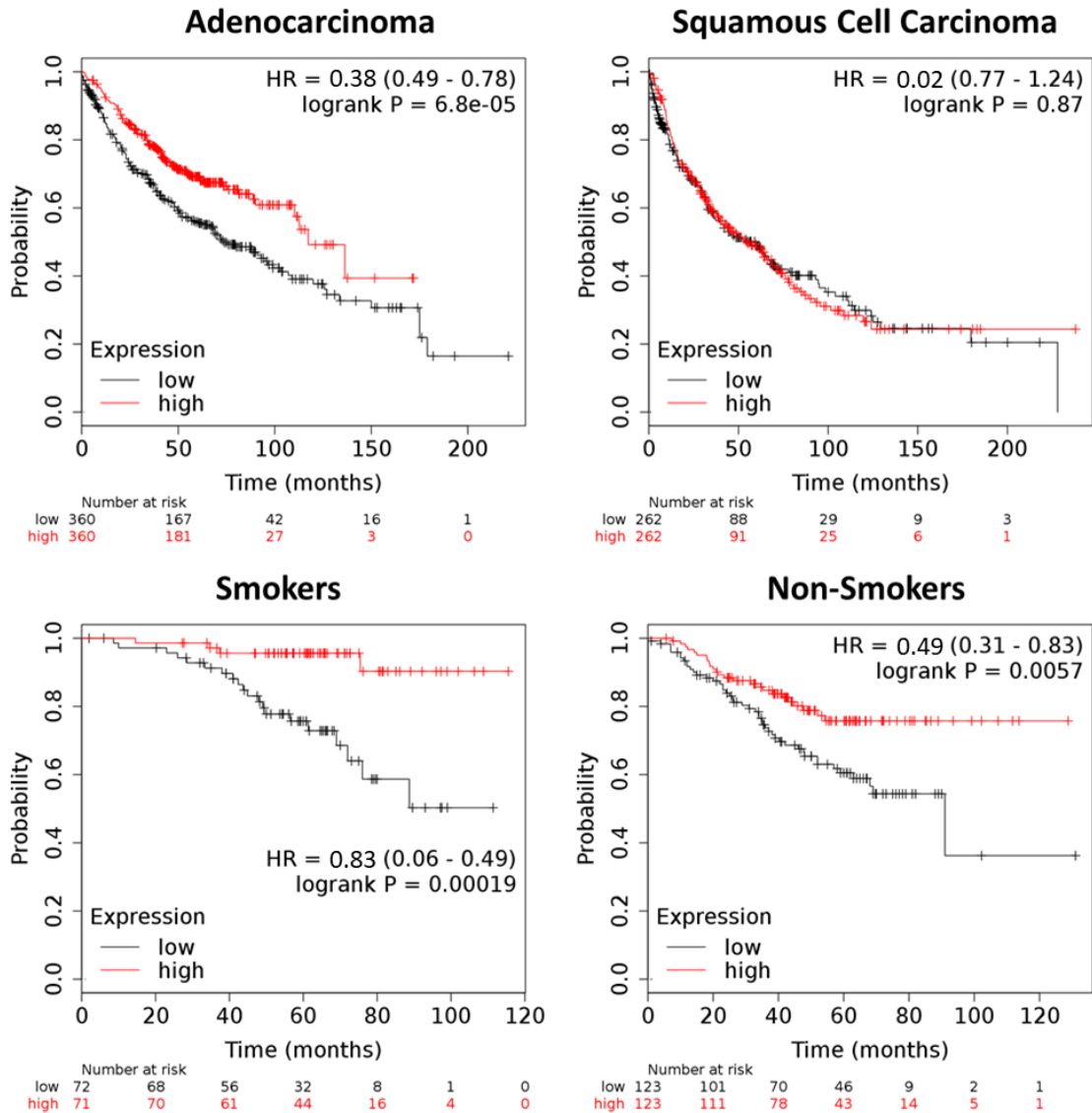


Figure 3.1 Low PRP4K predicts worse overall survival in lung adenocarcinoma patients. Overall survival in 524 (LUSC) or 719 (LUAD) lung cancer patients as well as LUAD smokers (n=246) and non-smokers (n=143) based on median expression of PRP4K was analyzed using microarray and survival data from <https://kmplot.com/analysis/index.php?p=service&cancer=lung>¹²¹. A smoker was defined as someone who currently smokes or has, non-smokers were defined as never smokers. HR = hazard ratio.

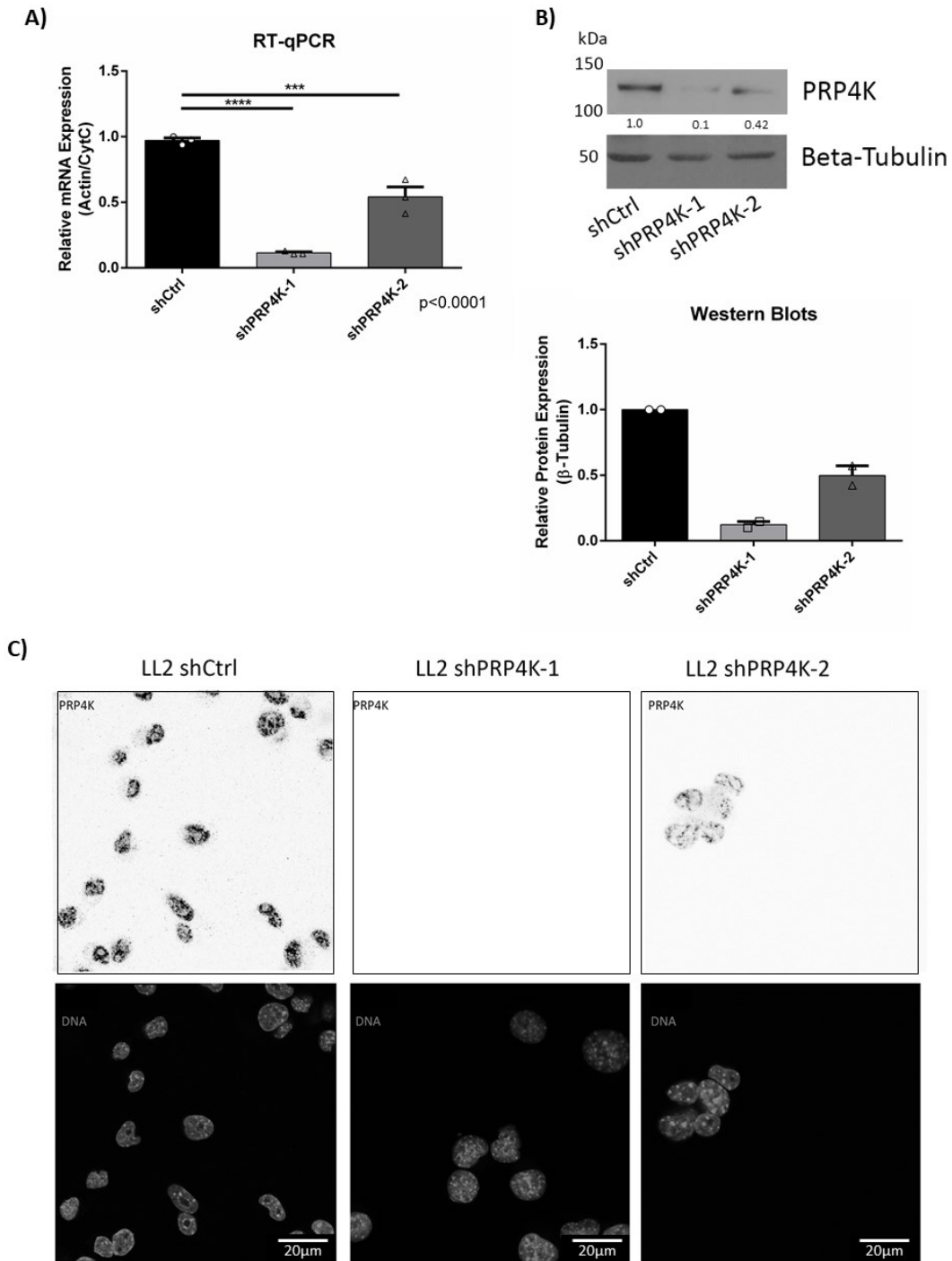


Figure 3.2 Validation of PRP4K knockdown in Lewis Lung Carcinoma cells (LLCs). Knockdown confirmation was validated three separate ways on different cell passages: (A) RT-qPCR (n=3), (B) Western Blot (n=2), and (C) Immunofluorescence microscopy. Statistical significance was determined using a one-way ANOVA with Tukey's post-hoc test and error bars represent SEM; *** $p < 0.001$, **** $p < 0.0001$.

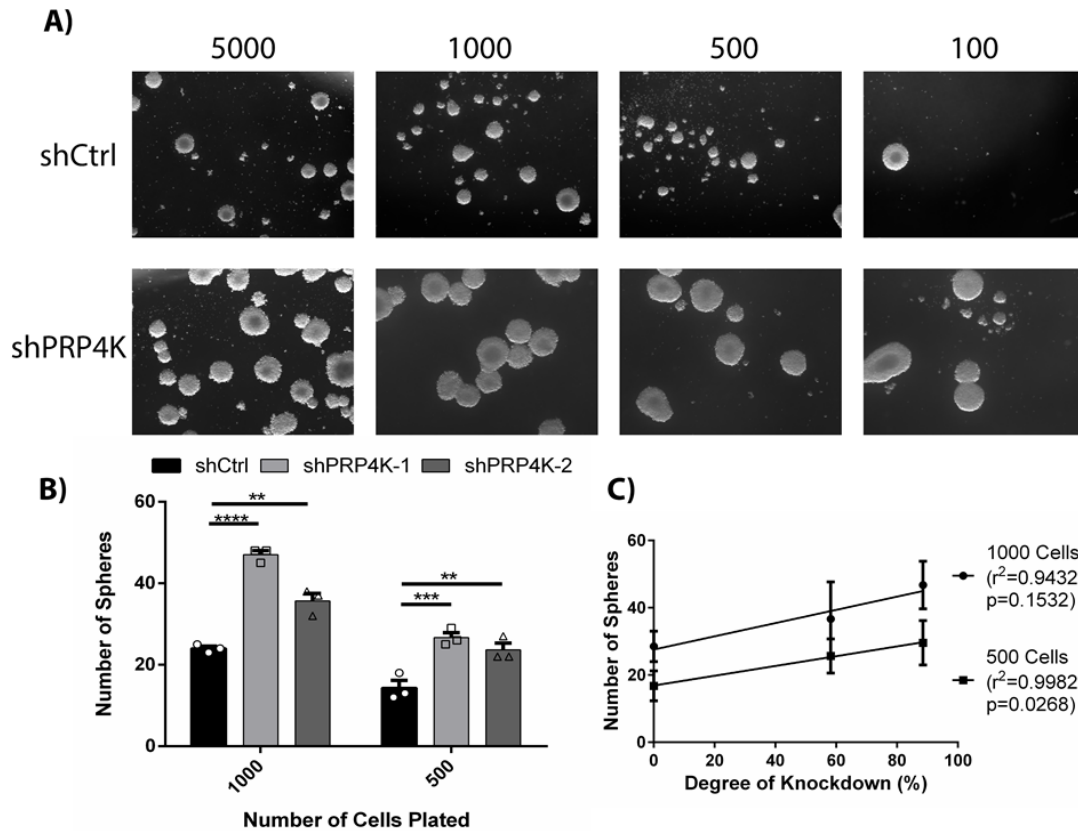


Figure 3.3 Knocking down PRP4K results in increased tumorsphere formation. Cells were plated at the indicated densities in cancer stem cell media for six days prior to counting using an inverted microscope. Representative images are shown under 12x magnification (**A**) and quantified ($n=3$; **B**). (**C**) Correlation between degree of knockdown (by RT-qPCR) and number of spheres formed. Statistical significance was determined using one-way ANOVAs with Tukey's post-hoc test and error bars represent SEM; ** $p<0.01$, *** $p<0.001$, **** $p<0.0001$.

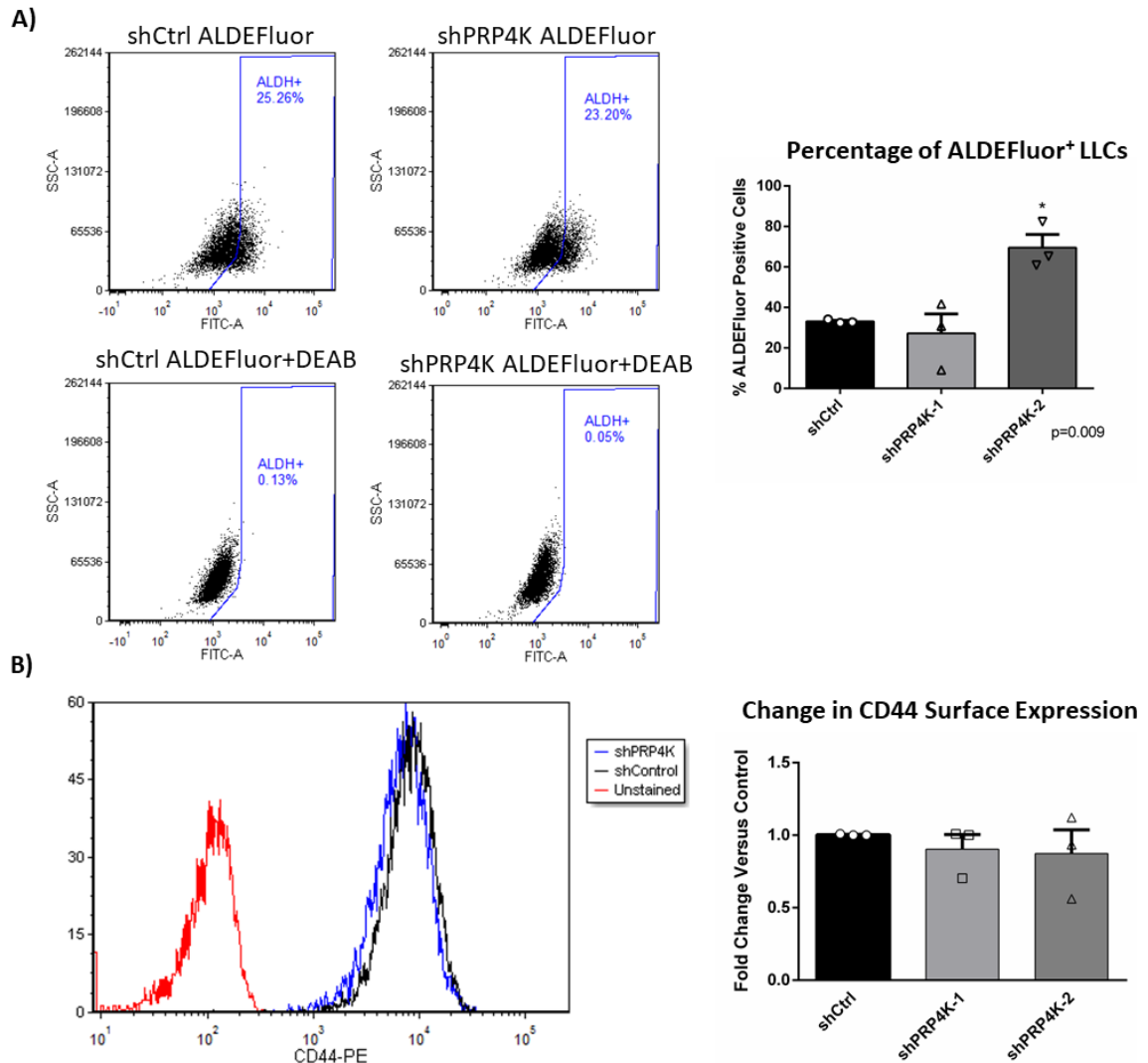


Figure 3.4 PRP4K knockdown does not affect the ALDH or CD44 CSC populations in LLCs. (A) Flow cytometry was used to quantify changes in ALDEfluor activity. Representative FACS plots of cell populations that are ALDH⁺ are shown. The inclusion of a DEAB-treated control allows for proper gate setting during FACS (n=3). (B) Flow cytometry was used to quantify changes in CD44 surface staining. Representative histograms of CD44-PE are shown. Unstained controls were used to ensure proper gating during FACS (n=3). Statistical significance was determined using a one-way ANOVA with Tukey's post-hoc test and error bars represent SEM; *p<0.05.

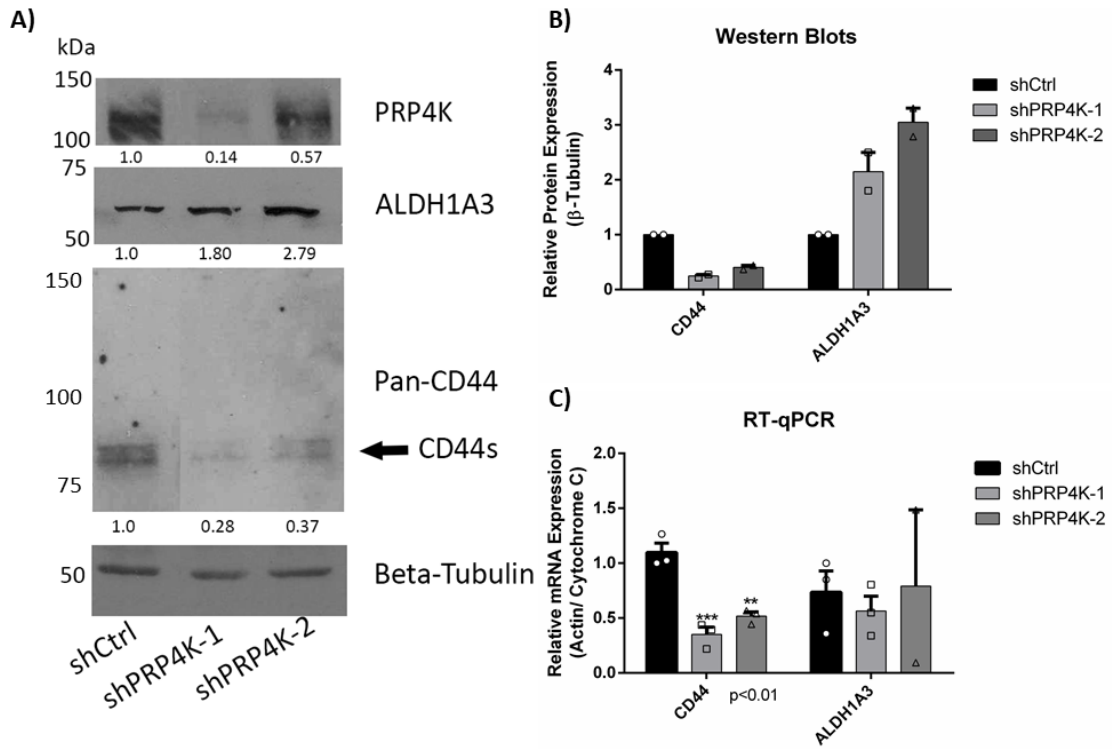


Figure 3.5 Further analysis of CSC markers in LLCs. Western Blot analysis of CSC markers (**A**) as well as the quantification of these markers (**B**; n=2). (**C**) RT-qPCR analysis of CD44 and ALDH1A3 transcript levels. Statistical significance was determined using a one-way ANOVA with Tukey's post-hoc test and error bars represent SEM; **p<0.01., ***p<0.001.

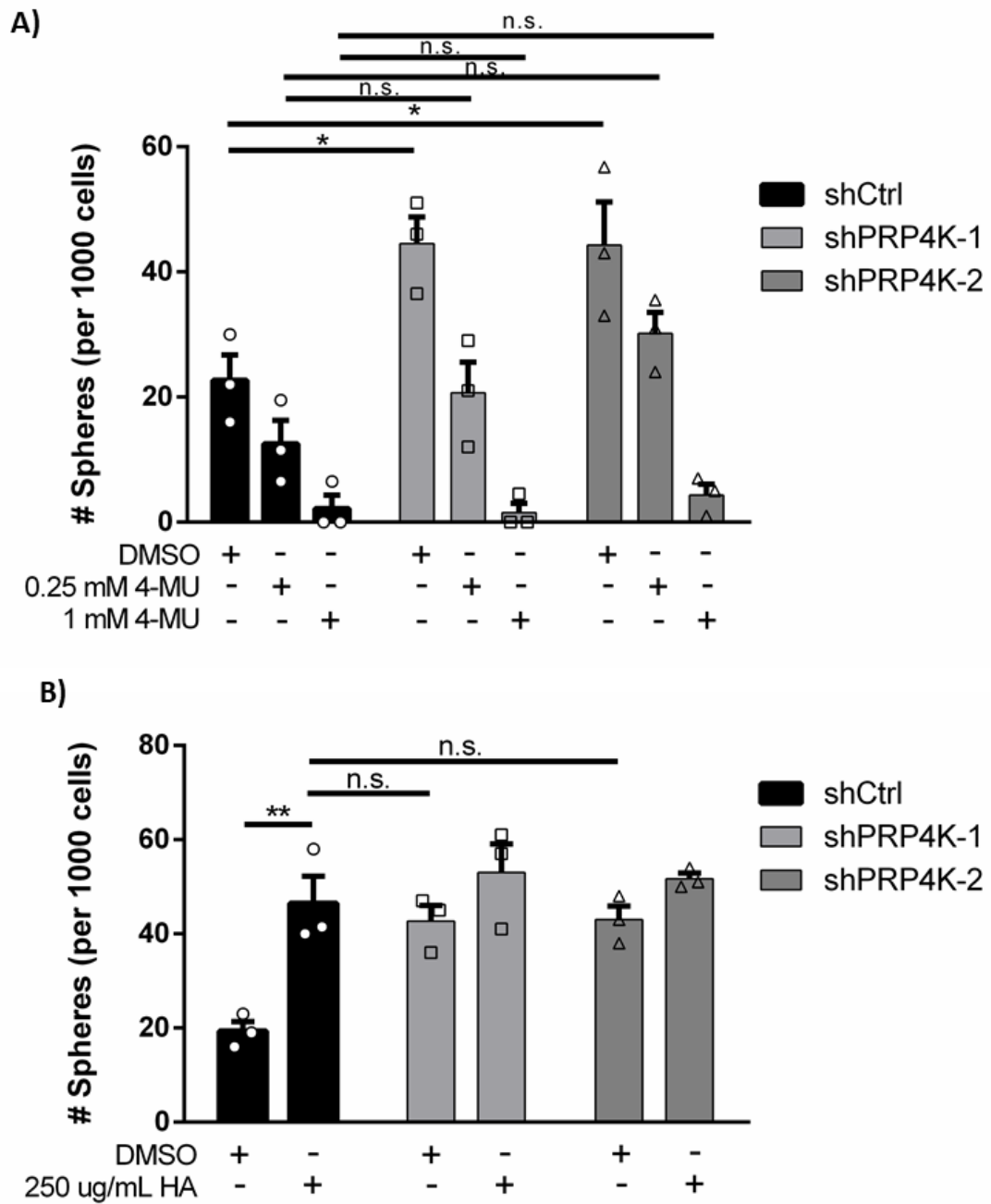


Figure 3.6 PRP4K Knockdown exerts its effects in part through hyaluronic acid. LLCs tumorspheres were incubated with the indicated treatments for 6 days in CSC media prior to counting (A). (B) LLC tumorspheres were incubated with or without HA and quantified after 6 days in CSC media. Significance determined using a two-way ANOVA with multiple comparisons and error bars represent SEM; * $p < 0.05$, ** $p < 0.01$.

3.2 Feature of Epithelial-to-Mesenchymal transition (EMT) are Associated with Depletion of PRP4K in the Mouse Lewis Lung Carcinoma model

Given that EMT and stemness are closely linked (See section 1.4 above), I wanted to determine whether knocking down PRP4K caused any changes to EMT-related genes. To do this, I performed Western Blots for common EMT genes. I found that knocking down PRP4K resulted in an almost complete loss of fibronectin, and a decrease in vimentin expression (both of which are mesenchymal markers), with an increase in the expression of EMT transcription factor Snail (Figure 3.7 A and B). The epithelial marker E-cadherin was not detected in these lines suggesting they exist in a mesenchymal, or hybrid EMT state prior to PRP4K knockdown. To determine whether these changes are transcriptional or translational, I used RT-qPCR to look at transcript levels of these genes, and found that both fibronectin *and* vimentin are being regulated at the gene expression level, while its likely that snail and slug are undergoing post-transcriptional control (Figure 3.7 C). Interestingly, while I was unable to detect any E-cadherin protein, I did in fact detect a transcript, albeit at an extremely low level ($C_t > 35$).

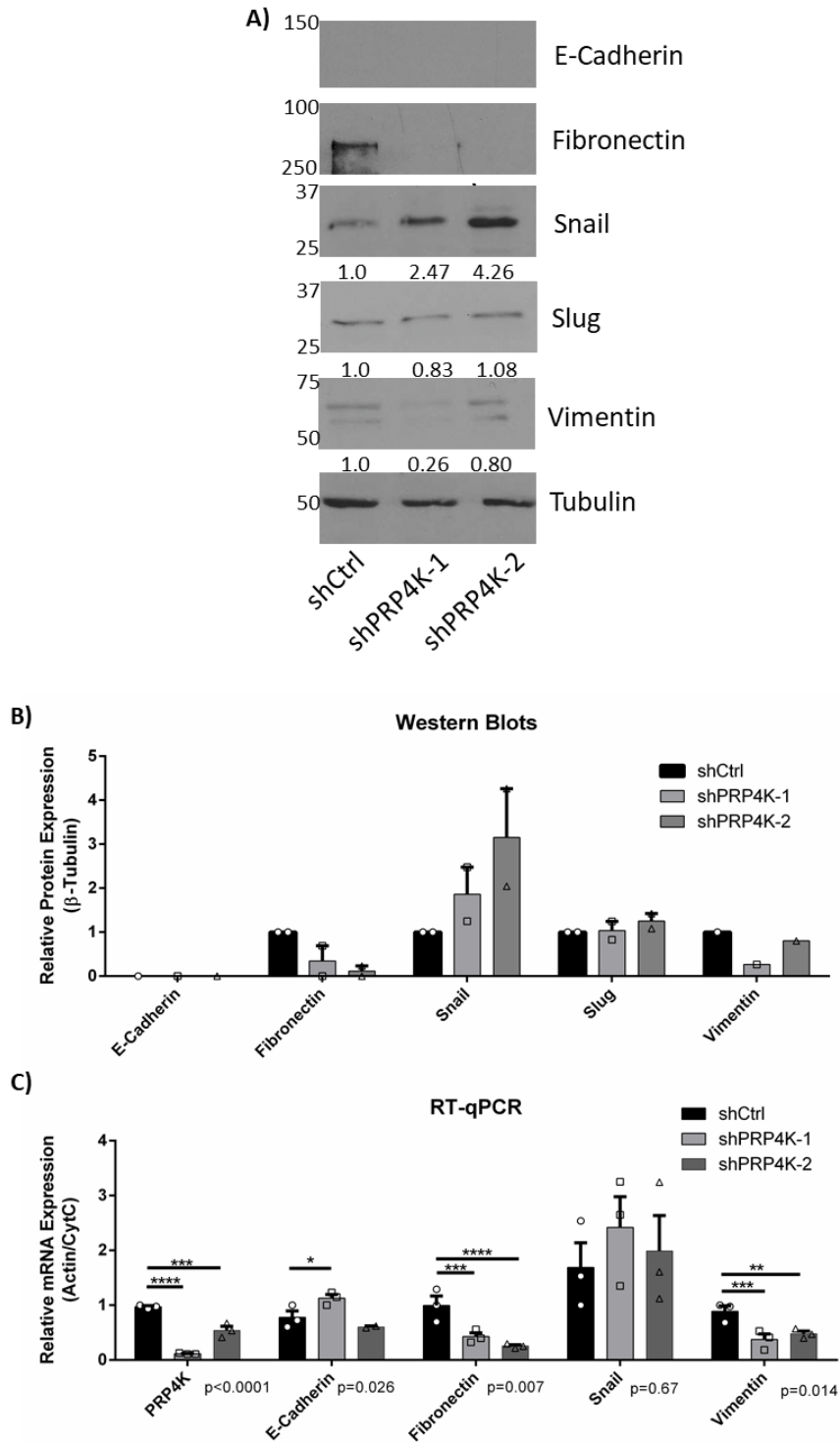


Figure 3.7 Knockdown of PRP4K affects levels of EMT-related genes in LLCs. (A) Western Blot analysis of EMT genes affected by PRP4K; (B) Quantification of Western Blots from panel (A; n=2); (C) mRNA levels of the genes from panels (A) and (B; n=3). Significance was determined by one-way ANOVA with Tukey's post-hoc, error bars represent SEM. * $p < 0.05$, ** $p < 0.01$, *** $p < 0.001$, **** $p < 0.0001$.

3.3 PRP4K Knockdown Promotes RA Resistance

Since I've already established that knocking down PRP4K results in an increased number of CSCs in LLCs and that RA is used to differentiate CSCs, I was interested as to whether my KDs were more susceptible to treatment with RA. To characterize the response, I looked at three different phenotypes: differentiation (by tumorsphere assay), proliferation, and gene expression changes. I found that the shCtrl line responded to RA by forming less tumorspheres (Figure 3.8A; ~55% less), proliferating more slowly (Figure 3.9; ~55% less cells at 72 hrs), and by inducing the expression of both RAR β and Crabp2 (Figure 3.8B). The knockdowns, on the other hand showed either no change to differentiation/ proliferation or less of an inhibition (~30% decrease in shPRP4K-2 versus 55% in the shCtrl). Gene expression changes, however, still occurred but to a lesser degree than was seen in the shCtrl cells, which is consistent with the other two phenotypes (Figure 3.8).

I next sought to determine the mechanism behind this and started by looking at the retinoic acid binding proteins, Crabp1 and Crabp2, which carry RA from the cytoplasm into the nucleus. I found that mRNA levels of both proteins were decreased with PRP4K knockdown (p=0.04 and p=0.06, respectively) and this correlated with a decrease in Crabp1 protein levels by Western Blot (Figure 3.10). Since RA can also bind to the fatty acid binding protein Fabp5 as well as the retinoic acid receptor RAR β , I also looked at these and while I found no change in Fabp5 levels, I did see a decrease in RAR β expression in one of the shRNAs.

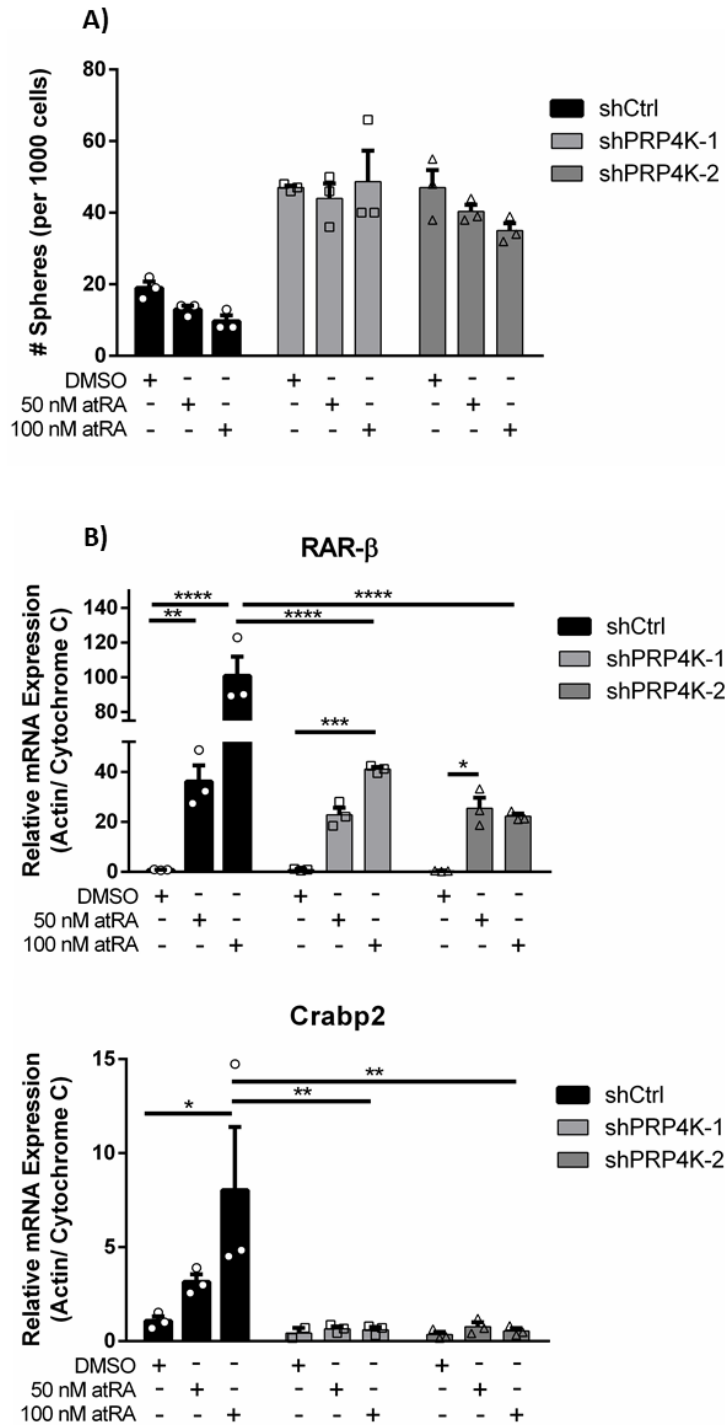


Figure 3.8 PRP4K Knockdown reduces sensitivity to RA-induced differentiation and gene expression induction in LLCs. (A) Tumorsphere formation of shCtrl and shPRP4K LLCs treated with the indicated compounds. (B) RT-qPCR was used to examine the induction of RA-inducible genes. Three reference genes were tested and the two most stable were selected. For all RA experiments, cells were continuously exposed to the indicated dose. Significance was determined using a two-way ANOVA, error bars represent SEM. * $p < 0.05$, ** $p < 0.01$, *** $p < 0.001$, **** $p < 0.0001$.

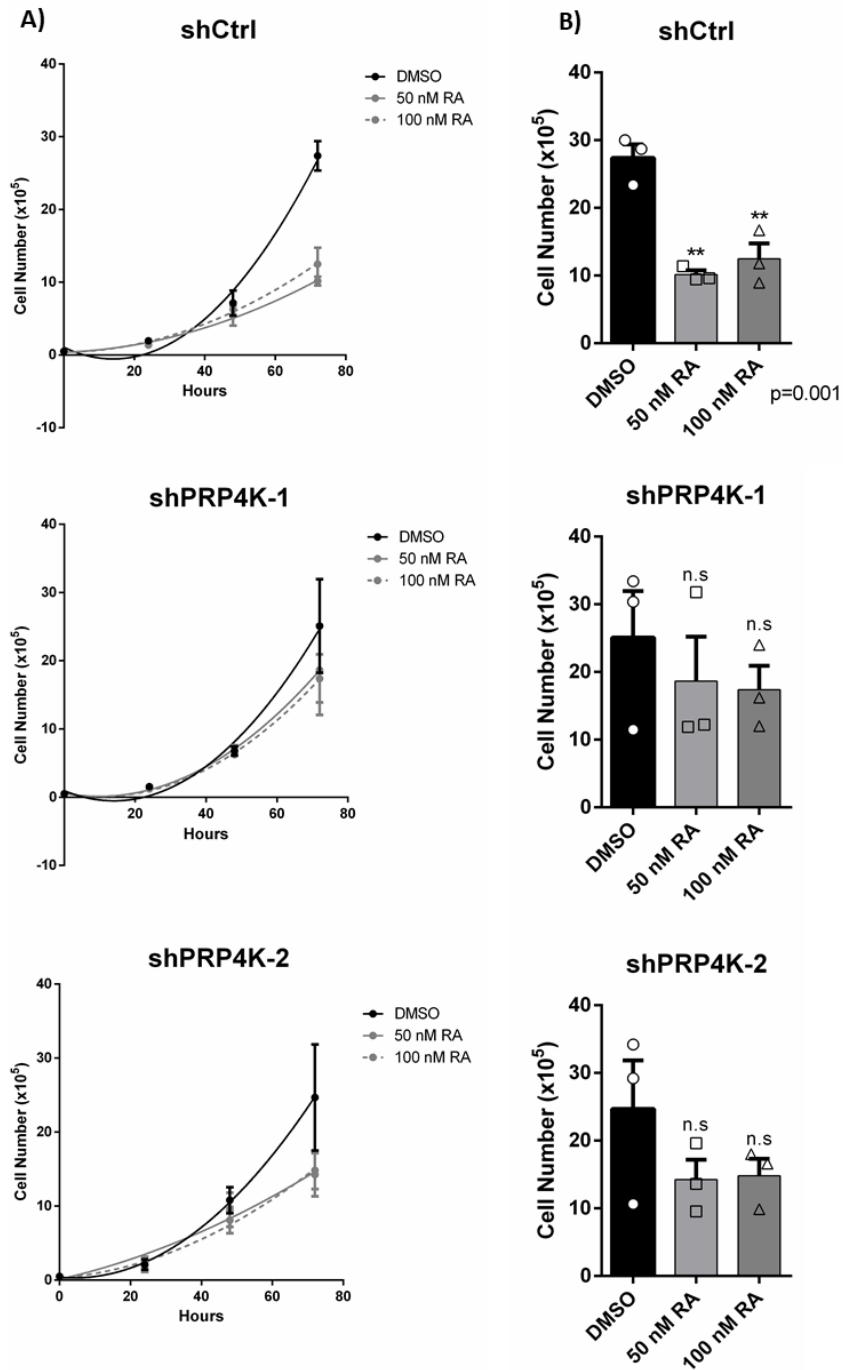


Figure 3.9 PRP4K knockdown reduces sensitivity to RA-induced proliferation inhibition in LLCs. (A) 5×10^4 cells were plated into 6-well plates and cells were counted every day for three days in the presence or absence of RA ($n=3$). (B) Number of cells after 72 hrs in RA ($n=3$). Significance was determined using a one-way ANOVA with Tukey's post-hoc test, error bars represent SEM. ** $p < 0.01$.

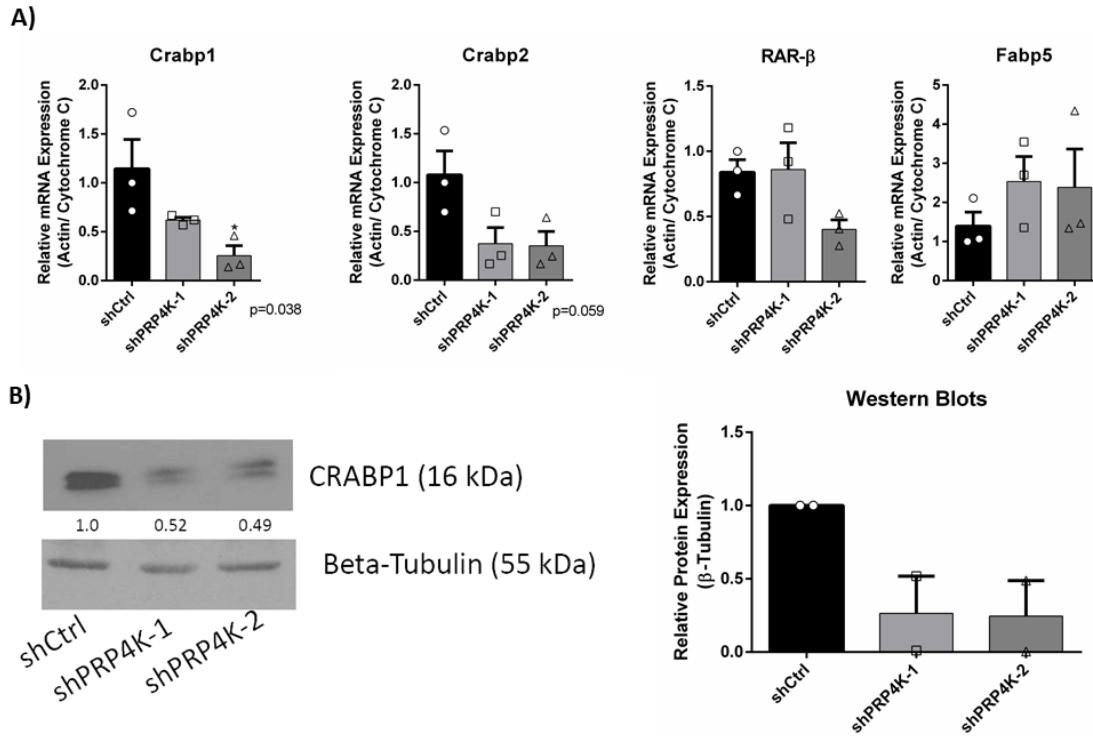


Figure 3.10 PRP4K Knockdown decreases the expression of RA binding proteins in LLCs. (A) Basal levels of RA binding proteins were examined by RT-qPCR (n=3) as well as the protein level of Crabbp1 by Western Blot (n=3; B). Significance was determined by a one-way ANOVA and error bars represent SEM; *p<0.05.

3.4 PRP4K Knockdown Increases Tumor Growth *in vivo* in the Mouse Lewis Lung Carcinoma Model

To assess the impact of PRP4K knockdown on tumor growth *in vivo*, I first performed a preliminary experiment, whereby 5×10^5 LLCs were injected subcutaneously into the left flank of C57BL/6 mice (For experimental layout, see Figure 2.2 A). For this experiment, I only used one control shRNA and one shPRP4K, and what I found was that the knockdown developed tumors much quicker than the controls (day 11 versus day 17), they grew quicker ($p < 0.0001$; Figure 3.11 A), and the tumors weighed more at the end of the experiment ($p = 0.0008$; Figure 3.11 B). I also removed one of the lungs, mechanically dissociated it, and plated it in a six-well plate for ~two weeks to determine whether the tumors had metastasized to the lungs. Consistent with a partial EMT phenotype, I saw that the mice that had received PRP4K knockdown cells had significantly more metastatic nodules in the lungs by both clonogenic assay ($p = 0.03$; Figure 3.11 C and D), as well as visually by histology (Figure 3.11 E).

The follow-up experiment to this was larger, consisting of two different control shRNAs and two different PRP4K shRNAs. This time, however, I was just interested in tracking tumor size and survival. Given that the two control shRNAs were behaving very similarly, the data were combined to simplify the analysis and clarify the graphs. What I found was that the PRP4K knockdowns again formed tumors earlier and grew more quickly ($p < 0.0001$; Figure 3.12 A) but didn't show different survival rates (Figure 3.12 B).

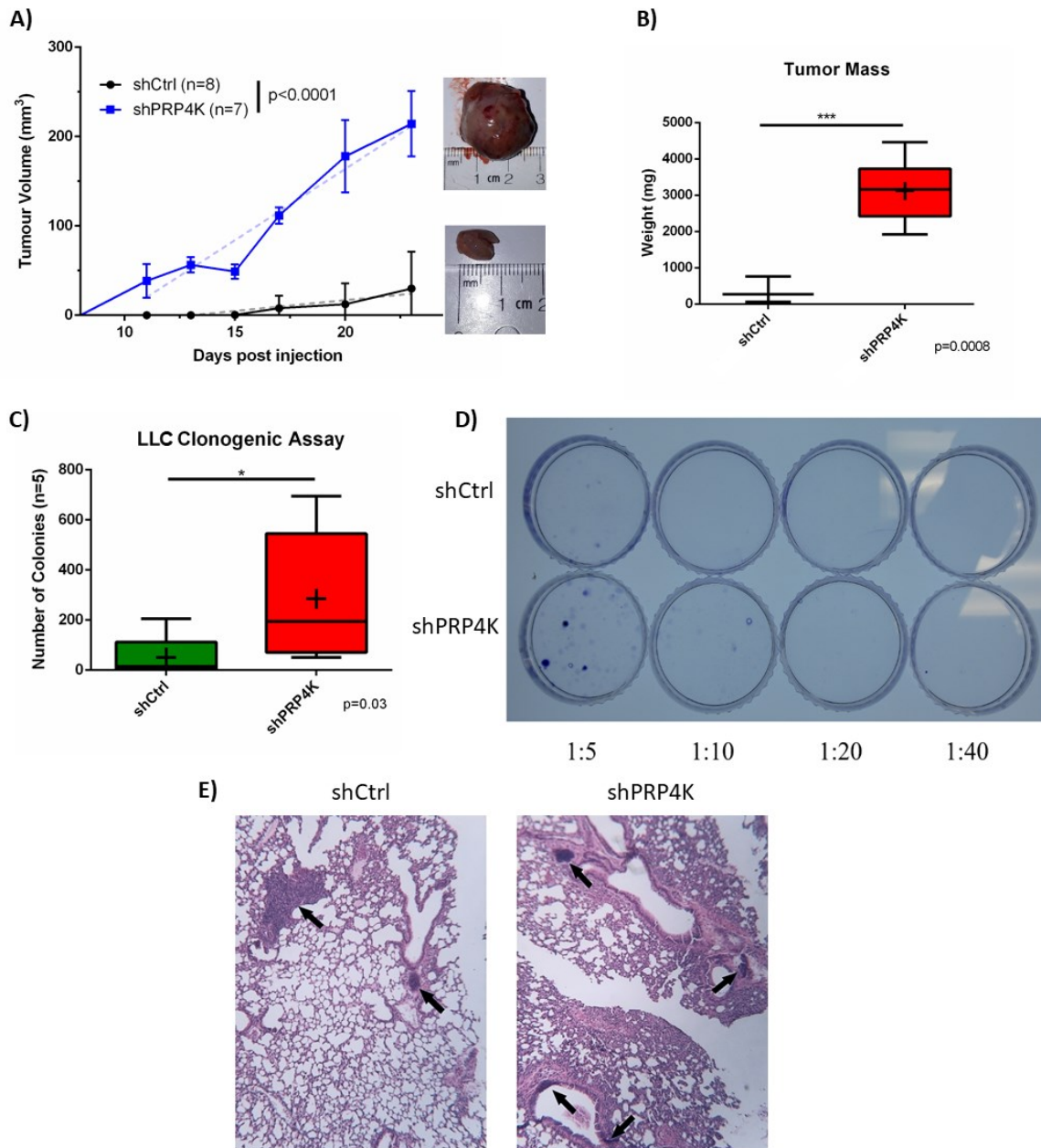


Figure 3.11 PRP4K knockdown affects tumor growth and metastasis *in vivo*. PRP4K knockdown resulted in quicker tumor growth (A), larger tumors (B), and increased metastasis to the lung as determined by clonogenic assay (C, D), and histological analysis under 40x magnification (E). Growth differences were determined by linear regression and weight/ colony number by two-tailed t-test. * $p < 0.05$, *** $p < 0.001$.

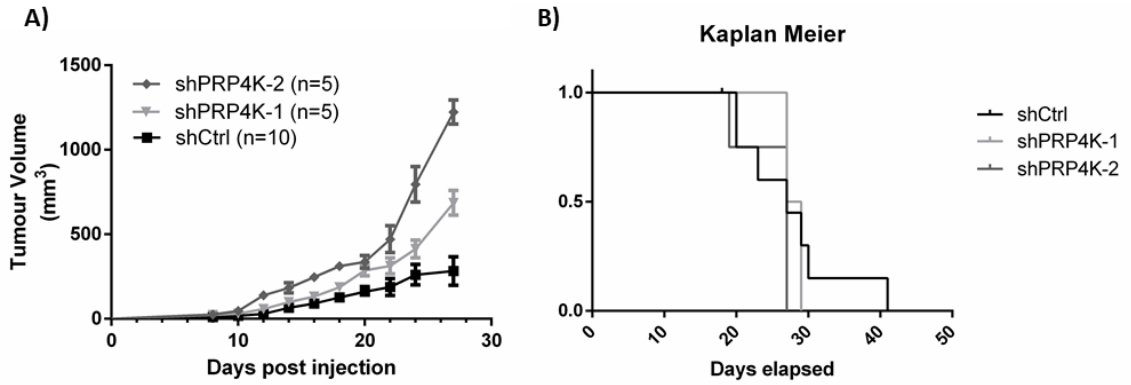


Figure 3.12 PRP4K knockdown affected tumor growth but not overall survival in C57BL/6 mice. Knocking down PRP4K resulted in increased tumor size ($p < 0.0001$; **A**) but had no significant effect on overall survival ($p = 0.43$; **B**).

Chapter 4: Discussion

4.1 Evidence of PRP4K as a Tumor Suppressor

In recent years, PRP4K has been increasingly studied for its role as a tumor suppressor, however the results of these study have been largely contradictory. For example, Corkery et al. (2015) found that PRP4K knockdown reduced cells' sensitivity to taxanes, which is consistent with what I found here, wherein PRP4K knockdown reduced sensitivity to RA¹²⁰. In contrast to this, Duan et al. (2009), showed that PRP4K knockdown actually sensitized cells to taxanes when examined using the same cell lines¹²². Corkery et al. (2018) also found that knocking down PRP4K promoted metastasis in the ID8 model of ovarian cancer and resulted in increased expression of the mesenchymal marker TrkB and that the metastatic nodules from the shCtrl group had decreased PRP4K and increased vimentin¹¹⁷. Taken together, these findings suggest the involvement of PRP4K in EMT and metastasis, which is again consistent with what I found here. Another group found that, in the MDA-MB-231 model of human triple negative breast cancer, PRP4K knockdown resulted in increased cellular proliferation, increased wound healing, and increased invasion *in vitro* and does so in a YAP-dependent manner¹²³. Conversely, Koedoot et al. (2019), using the same cell line, found the opposite result, with PRP4K knockdown reducing metastasis and slowing wound healing¹²⁴. Further evidence for the role of PRP4K as an oncogene was shown by Islam et al. (2018) in colon cancer, who also found that PRP4K overexpression actually reduced the expression of E-Cadherin and inhibited invasion¹²⁵. Gao et al. (2013) further showed that knocking down PRP4K in breast and pancreatic cancer decreased cellular viability in a kinase-dependent manner¹²⁶. Taken together, these data suggest that the role of PRP4K in tumor suppression is still

being determined as there seems to be a large amount of variation between different labs even when using the same cell line. This may be due to both intra- and interlaboratory variation caused naturally by mutations occurring in cancer cells or by using slightly different culture conditions. This has been previously shown by Ben-David et al. (2019), who found significant expression variations between strains of MCF10A, MCF7, and A549 cells both within and between labs¹²⁷. It's also possible that short-term (i.e. acute) and long-term (i.e. chronic) knockdown may be producing different effects.

4.2 Stemness

Given the poor survival rate of lung cancers, and the fact that PRP4K levels can be predictive of overall survival (Figure 3.1), I wanted to determine what role it was playing in these cancers. Based on the previous literature studying low PRP4K, which showed chemotherapy resistance, anoikis resistance, increased metastasis, and unpublished data from the lab showing partial EMT, I was interested in its role in stemness^{117,120}. Utilizing the Lewis Lung Carcinoma cell line, I was able to show that knocking down PRP4K using two different shRNAs caused cells to behave more stem-like (i.e. increased tumorsphere formation) versus those containing a non-targeting shRNA (Figure 3.2), but got conflicting results when repeating the anoikis resistance phenotype (Appendix 1A). This stemness phenotype tracked *in vivo*, wherein the shPRP4K tumors developed more quickly and grew faster. To further elucidate the mechanism behind this phenotype, I started by examining the expression of the two most common CSC markers: CD44 and ALDEFluor. In both knockdown lines, ALDH1A3 protein was increased but, in the LLC shPRP4K-2 line, ALDH1A3 protein levels were highest, while the transcript levels were unaffected, suggestive of increased translation of this protein. This correlated with

increased ALDEFfluor activity in the shPRP4K-2 line, but not in the shPRP4K-1 line. Furthermore, the surface expression of CD44 was not affected by PRP4K knockdown, however, total CD44 was decreased as was the CD44 transcript. Together, this indicates that CD44 may be downregulated transcriptionally, but the receptors on the surface of the cell are potentially not being endocytosed by knockdown of PRP4K. It should also be noted that emerging research in this field is beginning to demonstrate that the ALDH⁺ and the CD44⁺ CSC populations may in fact be two separate populations of cells. It has recently been shown in A549 cells (a KRAS mutated human lung adenocarcinoma cell line) that the CD44^{low} population actually forms larger tumors and shows decreased sensitivity to docetaxel (a taxane analog) when compared to the CD44^{high} population⁹⁸. To examine how these populations relate to one another, I wanted to determine how knocking down PRP4K affected the various LCSC populations. The results demonstrated that knocking down PRP4K didn't affect the overall distribution of these populations, with most of them being CD44^{high}/ALDH^{high} (Appendix 1B). Another important note for this cell line is that all of them are CD44⁺, suggesting it probably isn't the best marker for stemness in this case. Furthermore, these experiments were all performed on adherent cells, but culturing cells under non-adherent conditions (i.e. as tumorspheres) may induce the expression of different genes in my shCtrl versus shPRP4K cells. For example, while it has been shown that ALDH1A3 is the main contributor to ALDEFfluor activity in LCSCs (under adherent conditions), it has also been found that ALDH1A1 is significantly upregulated when lung cancer cells (both cell lines and patient samples) are cultured under non-adherent conditions^{79,128}. For this reason, it is probably worth examining the effects of PRP4K knockdown in these cells when cultured as spheres and

compare that to expression changes when cultured as a monolayer. The ideal next experiments for this part of the project would be to repeat this in another cell line (preferably human) and take the limiting dilution assays *in vivo* using both immunocompetent mice (C57BL/6) and immunocompromised mice (e.g. NOD/SCID) to determine the involvement of an immune system in mediating my phenotypes.

4.3 Hyaluronic Acid

Given this stemness phenotype and the lack of changes in these CSC markers, I next wanted to investigate the role of hyaluronic acid (the primary ligand for CD44) in the context of PRP4K knockdown. I first decided to treat my cells with an HA synthesis inhibitor to determine what effect that had on my phenotype. I found that the shPRP4K cells were more sensitive to the inhibitor than the shCtrl cells, and that I was able to mimic the phenotype of the LLC shPRP4K cells in the shCtrl cells by exposing them to exogenous HA (250 µg/mL). It should also be noted that the HA used was of a medium-high molecular weight, which may be inhibitory to cell growth, but since the cells grew better, it's likely that both the shCtrl cells *and* the shPRP4K cells have a high expression of hyaluronidases (enzymes responsible for cleaving HA into smaller fragments)¹⁰⁰. Determining the levels of HA synthesis (by ELISA) would be the next step, as well as looking at the expression of HAS genes/ proteins.

4.4 EMT

Given the known relationship between stemness and EMT, as well as the data the lab has on PRP4K and EMT, I decided to see how this applied to my model. I found that

knocking down PRP4K in LLC cells resulted in a striking decrease in both protein and mRNA levels of the mesenchymal markers fibronectin and vimentin. I also saw an increase in protein expression of the EMT transcription factor Snail with no change in mRNA expression (suggesting post-transcriptional regulation). When taken *in vivo*, preliminary data suggests that PRP4K knockdown cells are more metastatic, as evidenced by increased nodules in the lung. There are a couple of methods commonly used *in vitro* to analyze EMT phenotypically, namely transwell assays, which test the ability of cells to migrate from a serum-free to serum-high environment. The inserts used for these assays can also be covered with Matrigel to test cells' invasive ability. A preliminary experiment using one shCtrl and one shPRP4K was performed, however, there were no differences in either the migration *or* invasion assays (Appendix 1C). As previously mentioned, the existence of hybrid EMT states is well known but there are some things that need to be kept in mind when undertaking this research. Due to the fact that cell lines can be sorted into different populations based on the differential expression of various EMT markers, it is important to remember that when looking at unsorted cells, it may appear as though cells are in a partial-EMT state (indicated by the presence of both epithelial *and* mesenchymal markers), when in reality there are simply two distinct populations of cells (one epithelial and one mesenchymal). In the current study, I only examined cells at a population level by Western Blotting, which means I am only seeing the average expression of these markers. A more in-depth method for examining hybrid EMT states would include the use of techniques such as immunofluorescence microscopy or flow cytometry, both of which are able to give single-cell resolution.

4.5 Retinoic Acid

When it comes to CSCs, there are few treatments known to target them, but one of the most common is retinoic acid. Since knocking down PRP4K increased the number of CSCs, I wondered if they would be more susceptible to treatment with *all-trans* retinoic acid (RA). This was not the case, in fact, they were less sensitive, or didn't respond at all. As previously mentioned, RA eliminates CSCs using two different mechanisms: cell cycle arrest (leading to apoptosis), as well as induction of differentiation and does so by activating transcription of genes involved in regulating these pathways. In the shCtrl cells, I saw a decrease in differentiation and proliferation, however, this was not the case when PRP4K was knocked down. Upon doing RT-qPCR on RA treated cells, I noticed that my shPRP4K cells were not inducing RA-inducible genes to the same extent as my shCtrl cells. To me, this suggested that RA was most likely not making it into the nucleus, so I decided to look at the expression of the retinoic acid binding proteins Crabp1 and Crabp2. As it turned out, knocking down PRP4K decreased both the mRNA *and* protein levels of Crabp1 as well as mRNA levels of Crabp2, suggesting that the decrease in sensitivity is most likely due to the RA not being translocated into the nucleus. Crabp1 was also determined to be decreased in my proteomics datasets (data not shown). This is not the first time that low levels of Crabp1 have been associated with lowered response to RA, in fact, it has been shown that cancer cells lacking Crabp1 fail to undergo RA-induced apoptosis, and that re-expressing Crabp1 in these lines re-sensitizes them to RA¹²⁹. Crabp2 has also been studied as a putative tumor suppressor. One study showed that low Crabp2 was associated with increased lymph node metastasis in NSCLC, while another showed that low Crabp2 is associated with increased metastasis,

increased viability, and progression through the cell cycle in esophageal squamous cell carcinoma^{130,131}. In ER⁺ breast cancers, low Crabp2 has also been associated with partial induction of EMT (less E-cadherin, more vimentin), and increased metastasis to the lung¹³². One method for determining whether or not this lack of translocation is the cause would be to use fluorescently tagged RA to track its translocation with PRP4K knockdown¹³³. Further experiments for this project would include taking this *in vivo* and using slow release RA pellets as well as doing Crabp1 overexpression in PRP4K KD cells to try and reverse the phenotype. It's also important to note that RA treatments were performed in carbon stripped FBS, to ensure that no other retinoids were present during treatments.

4.6 Limitations

One limitation of this study is that in many cases, the two hairpins used to knockdown PRP4K in a cell line did not show consistent proteomic and/or metabolomic changes. The shRNA RNA interference technology does have significant off-target effects¹³⁴. Unfortunately, it was not possible to simply knock-out the PRP4K gene *PRPF4B* due to its essentiality for cell division and pre-mRNA splicing^{113,135}. In the future, the recently developed CasRX system developed by Konermann and colleagues could be used to effectively “knock-out” the transcript of the gene of interest. The CasRX system was found to outperform shRNA, displaying a knockdown of ~96%, in comparison to the 65% knockdown by shRNA. Most importantly, the CasRX system showed no significant off-target effects, which is a huge concern and downfall of the currently used techniques to knockdown genes. For example, Konermann et al. show that the KD of annexin A4 (*ANXA4*) by shRNA causes over 900 significant off-target

transcript changes as opposed to the CasRX system, which exhibited no significant off-target gene expression changes when used to target the same gene¹³⁴. Another potential method that could be used for generating knockdowns would be through the use of an auxin-inducible degron (AID) system. In this system, an auxin receptor is CRISPR knocked-in to the endogenous locus of the gene of interest, and upon the addition of a compound from the auxin class (e.g. Indole-3-Acetic acid), the receptor interacts with a ubiquitin ligase (TIR1), which ubiquitinates the target protein and targets it for proteasomal degradation^{136,137}. This allows for rapid (~90% knockdown within one hour) and dosable knockdowns with no off-target effects, and since auxins aren't found in human cells, there is no worry of basal degradation. The auxin receptor may also be combined with a fluorescent tag and/or nuclear localization signals (NLS) to further modify proteins of interest¹³⁸.

The cell line used here was the Lewis Lung Carcinoma cell line, which is one of the only syngeneic mouse models of lung cancer commercially available. The only other one available for C57BL/6 mice are the CMT167 and CMT64 cell lines (highly metastatic and non-metastatic, respectively) and are subclones derived from the same tumor¹³⁹. Since the LLC cells are non-metastatic, the CMT64 cell line would be the best model for me to use for repeating these phenotypes *in vivo*. Another important consideration for these experiments is the driver mutation behind them. The LLCs harbor an activating KRAS^{G12C}, whereas the CMT cell lines harbor an activating KRAS^{G12V} mutation, thus the ideal human cell line would also harbor an activating KRAS mutation such as the H23 cell line which also have an activating KRAS^{G12C} mutation^{140,141}. Since these experiments were performed in immunocompetent mice, it would also be

interesting to repeat them in an immunocompromised mouse model to determine the importance of an immune system in mediating my phenotypes *in vivo*. The final consideration of these *in vivo* experiments is that I am injecting cells into the mouse, and having tumors develop within about a week. When I do this, however, I am missing the natural development of the tumor and how these early stages affect and are affected by the immune system. I also did my injections subcutaneously in the left flank, as opposed to doing them orthotopically (i.e. in the lung). Ideally, a smaller number of cells would be either injected into the alveoli, or inhaled by the mice, so that these cells end up in their natural niche. The major limitation of using mouse cell lines is that the results may not necessarily be the same when converted to human cells.

Chapter 5: Conclusions

In this thesis, I first determined that knocking down PRP4K in Lewis Lung Carcinoma cells conferred a stem-like phenotype (i.e. increased tumorsphere formation) on these cells. I then showed that this may be due to the PRP4K KD cells being in a hybrid EMT state and/or involve increased hyaluronic acid production (but not due to changes in CSC makers CD44 or ALDH1A3). I also determined that PRP4K KD cells are less sensitive (to differentiation, proliferation inhibition, and activation of gene expression) to the CSC-depleting chemotherapy *all-trans* retinoic acid via the transcriptional downregulation of Crabp1 and/or Crabp2. Taken together, the results of this study provide further evidence for the role of PRP4K as a tumor suppressor in non-small cell lung adenocarcinoma. A graphical summary of the data is shown below in Figure 6.1.

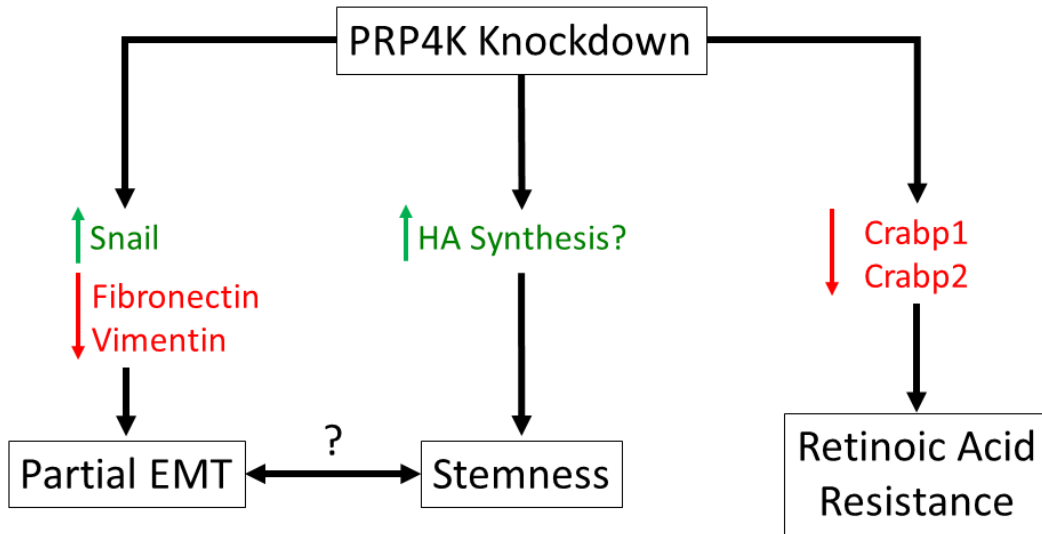


Figure 6.1 Graphical summary of the major findings from the current study.

References

1. Hassanpour SH, Dehghani M. Review of cancer from perspective of molecular. *J Cancer Res Pract.* 2017;4(4):127-129. doi:10.1016/j.jcrpr.2017.07.001
2. Faguet GB. A brief history of cancer: Age-old milestones underlying our current knowledge database. *Int J Cancer.* 2015;136(9):2022-2036. doi:10.1002/ijc.29134
3. Hassanpour SH, Dehghani M. Review of cancer from perspective of molecular. *J Cancer Res Pract.* 2017;4(4):127-129. doi:10.1016/j.jcrpr.2017.07.001
4. Hanahan D, Weinberg RA. The hallmarks of cancer. *Cell.* 2000;100(1):57-70. doi:10.1016/s0092-8674(00)81683-9
5. Hayflick L. The illusion of cell immortality. 2000;83(7):841-846. doi:10.1054/bjoc.2000.1296
6. Hanahan D, Folkman J. *Patterns and Emerging Mechanisms Review of the Angiogenic Switch during Tumorigenesis.* 1996(86).
7. Polyak K, Weinberg RA. Transitions between epithelial and mesenchymal states: acquisition of malignant and stem cell traits. *Nat Rev Cancer.* 2009;9(4):265-273. doi:10.1038/nrc2620
8. Levine AJ. P53, the Cellular Gatekeeper Review for Growth and Division. 1997(88).
9. Hanahan D, Weinberg RA. Hallmarks of cancer: the next generation. *Cell.* 2011;144(5):646-674. doi:10.1016/j.cell.2011.02.013
10. Vander Heiden MG, Cantley LC, Thompson CB. Understanding the Warburg Effect: The Metabolic Requirements of Cell Proliferation. *Science.* 2009;324(5930):1029-1033.
11. Wein-House S, Warburg O, Burk D, Schade AL. On Respiratory Impairment in Cancer Cells on JSTOR. *Science.* 1956;124(3215):267-272.
12. Harjes U. Embryonic factor helps tumours to lie low. *Nat Rev Cancer.* 2019;19(9):488-488. doi:10.1038/s41568-019-0191-z
13. Wang X, Teng F, Kong L, Yu J. PD-L1 expression in human cancers and its association with clinical outcomes. *Onco Targets Ther.* 2016;9:5023-5039. doi:10.2147/OTT.S105862

14. Garrido F, Aptsiauri N, Doorduijn EM, Garcia Lora AM, van Hall T. The urgent need to recover MHC class I in cancers for effective immunotherapy. *Curr Opin Immunol*. 2016;39:44-51. doi:10.1016/j.coi.2015.12.007
15. López-Novoa JM, Nieto MA. Inflammation and EMT: an alliance towards organ fibrosis and cancer progression. *EMBO Mol Med*. 2009;1(6-7):303-314. doi:10.1002/emmm.200900043
16. Aldinucci D, Colombatti A. The inflammatory chemokine CCL5 and cancer progression. *Mediators Inflamm*. 2014;2014:292376. doi:10.1155/2014/292376
17. Torre LA, Bray F, Siegel RL, Ferlay J, Lortet-Tieulent J, Jemal A. Global cancer statistics, 2012. *CA Cancer J Clin*. 2015;65(2):87-108. doi:10.3322/caac.21262
18. Molina JR, Yang P, Cassivi Stephen D, Schild SE, Adjei AA. Non-Small Cell Lung Cancer: Epidemiology, Risk Factors, Treatment, and Survivorship. *Mayo Clin Proc*. 2008;83(5):584-594. doi:10.4065/83.5.584
19. Sun S, Schiller JH, Gazdar AF. Lung cancer in never smokers — a different disease. *Nat Rev Cancer*. 2007;7(10):778-790. doi:10.1038/nrc2190
20. Network TCGAR. Comprehensive molecular profiling of lung adenocarcinoma. *Nature*. 2014;511(7511):543-550. doi:10.1038/nature13385
21. Ding L, Getz G, Wheeler DA, et al. Somatic mutations affect key pathways in lung adenocarcinoma. *Nature*. 2008;455(7216):1069-1075. doi:10.1038/nature07423
22. Pao W, Wang TY, Riely GJ, et al. KRAS Mutations and Primary Resistance of Lung Adenocarcinomas to Gefitinib or Erlotinib. Herbst R, ed. *PLoS Med*. 2005;2(1):e17. doi:10.1371/journal.pmed.0020017
23. Network TCGAR. Comprehensive genomic characterization of squamous cell lung cancers. *Nature*. 2012;489(7417):519-525. doi:10.1038/nature11404
24. Reck M, Rabe KF. Precision Diagnosis and Treatment for Advanced Non-Small-Cell Lung Cancer. Longo DL, ed. *N Engl J Med*. 2017;377(9):849-861. doi:10.1056/NEJMra1703413
25. Gajewski TF, Corrales L, Williams J, Horton B, Sivan A, Spranger S. Cancer Immunotherapy Targets Based on Understanding the T Cell-Inflamed Versus Non-T Cell-Inflamed Tumor Microenvironment. In: Springer, Cham; 2017:19-31. doi:10.1007/978-3-319-67577-0_2

26. Anichini A, Tassi E, Grazia G, Mortarini R. The non-small cell lung cancer immune landscape: emerging complexity, prognostic relevance and prospective significance in the context of immunotherapy. *Cancer Immunol Immunother.* 2018;67(6):1011-1022. doi:10.1007/s00262-018-2147-7
27. Lavin Y, Kobayashi S, Leader A, et al. Innate Immune Landscape in Early Lung Adenocarcinoma by Paired Single-Cell Analyses. *Cell.* 2017;169(4):750-765.e17. doi:10.1016/j.cell.2017.04.014
28. Kargl J, Busch SE, Yang GHY, et al. Neutrophils dominate the immune cell composition in non-small cell lung cancer. *Nat Commun.* 2017;8(1):14381. doi:10.1038/ncomms14381
29. Hanna N, Johnson D, Temin S, et al. Systemic Therapy for Stage IV Non–Small-Cell Lung Cancer: American Society of Clinical Oncology Clinical Practice Guideline Update. *J Clin Oncol.* 2017;35(30):3484-3515. doi:10.1200/JCO.2017.74.6065
30. Hirsch FR, Scagliotti G V, Mulshine JL, et al. Seminar Lung cancer: current therapies and new targeted treatments. *www.thelancet.com.* 2017;389. doi:10.1016/S0140-6736(16)30958-8
31. Goldstraw P, Chansky K, Crowley J, et al. The IASLC Lung Cancer Staging Project: Proposals for Revision of the TNM Stage Groupings in the Forthcoming (Eighth) Edition of the TNM Classification for Lung Cancer. doi:10.1016/j.jtho.2015.09.009
32. Kris MG, Gaspar LE, Chaft JE, et al. Adjuvant Systemic Therapy and Adjuvant Radiation Therapy for Stage I to IIIA Completely Resected Non-Small-Cell Lung Cancers: American Society of Clinical Oncology/Cancer Care Ontario Clinical Practice Guideline Update. *J Clin Oncol.* 2017;35. doi:10.1200/JCO.2017.72.4401
33. Herbst RS, Heymach J V., Lippman SM. Lung Cancer. *N Engl J Med.* 2008;359(13):1367-1380. doi:10.1056/NEJMra0802714
34. Soria J-C, Ohe Y, Vansteenkiste J, et al. Osimertinib in Untreated EGFR-Mutated Advanced Non–Small-Cell Lung Cancer. *N Engl J Med.* 2018;378(2):113-125. doi:10.1056/NEJMoal713137
35. Canon J, Rex K, Saiki AY, et al. The clinical KRAS(G12C) inhibitor AMG 510 drives anti-tumour immunity. *Nature.* 2019;575. doi:10.1038/s41586-019-1694-1
36. Herbst RS, Baas P, Kim D-W, et al. Pembrolizumab versus docetaxel for previously treated, PD-L1-positive, advanced non-small-cell lung cancer (KEYNOTE-010): a randomised controlled trial. *www.thelancet.com.* 2016;387. doi:10.1016/S0140-6736(15)01281-7

37. Borghaei H, Paz-Ares L, Horn L, et al. Nivolumab versus Docetaxel in Advanced Nonsquamous Non–Small-Cell Lung Cancer. *N Engl J Med*. 2015;373(17):1627-1639. doi:10.1056/NEJMoa1507643
38. Herbst RS, Sznol M. Diminished but not dead: chemotherapy for the treatment of NSCLC. *Lancet Oncol*. 2016;17(11):1464-1465. doi:10.1016/S1470-2045(16)30524-1
39. Reck M, Rodríguez-Abreu D, Robinson AG, et al. Pembrolizumab versus Chemotherapy for PD-L1–Positive Non–Small-Cell Lung Cancer. *N Engl J Med*. 2016;375(19):1823-1833. doi:10.1056/NEJMoa1606774
40. Al-Kattan K, Sepsas E, Fountain SW, Townsend ER. Disease Recurrence after Resection for Stage I Lung Cancer. *Eur J Cardiothorac Surg*. 1997; 12(3): 380-384. doi: 10.1016/s1010-7940(97)00198-x
41. Herbst RS, Morgensztern D, Boshoff C. The biology and management of non-small cell lung cancer. *Nature*. 2018;553(7689):446-454. doi:10.1038/nature25183
42. Molina JR, Yang P, Cassivi Stephen D, Schild SE, Adjei AA. Non-Small Cell Lung Cancer: Epidemiology, Risk Factors, Treatment, and Survivorship. *Mayo Clin Proc*. 2008;83(5):584-594. doi:10.4065/83.5.584
43. Kreso A, Dick JE. Evolution of the cancer stem cell model. *Cell Stem Cell*. 2014;14(3):275-291. doi:10.1016/j.stem.2014.02.006
44. Bonnet D, Dick JE. Human acute myeloid leukemia is organized as a hierarchy that originates from a primitive hematopoietic cell. *Nat Med*. 1997;3(7):730-737. doi: 10.1038/nm0797-730
45. Fang D, Nguyen TK, Leishear K, et al. A Tumorigenic Subpopulation with Stem Cell Properties in Melanomas. *Cancer Res*. 2005;65(20):9328-9337. doi:10.1158/0008-5472.CAN-05-1343
46. Collins AT, Berry PA, Hyde C, Stower MJ, Maitland NJ. Prospective identification of tumorigenic prostate cancer stem cells. *Cancer Res*. 2005;65(23):10946-10951. doi:10.1158/0008-5472.CAN-05-2018
47. Singh SK, Clarke ID, Terasaki M, et al. Identification of a cancer stem cell in human brain tumors. *Cancer Res*. 2003;63(18):5821-5828.
48. Dalerba P, Dylla SJ, Park I-K, et al. Phenotypic characterization of human colorectal cancer stem cells. *Proc Natl Acad Sci*. 2007;104(24):10158-10163. doi:10.1073/pnas.0703478104

49. Szotek PP, Pieretti-Vanmarcke R, Masiakos PT, et al. Ovarian cancer side population defines cells with stem cell-like characteristics and Mullerian Inhibiting Substance responsiveness. *Proc Natl Acad Sci U S A*. 2006;103(30):11154-11159. doi:10.1073/pnas.0603672103
50. Kim CFB, Jackson EL, Woolfenden AE, et al. Identification of Bronchioalveolar Stem Cells in Normal Lung and Lung Cancer. *Cell*. 2005;121(6):823-835. doi:10.1016/j.cell.2005.03.032
51. Li C, Lee CJ, Simeone DM. Identification of Human Pancreatic Cancer Stem Cells. *Methods Mol Biol*. 2009:161-173. doi:10.1007/978-1-59745-280-9_10
52. Chen K, Huang Y, Chen J. Understanding and targeting cancer stem cells: therapeutic implications and challenges. *Acta Pharmacol Sin*. 2013;34(6):732-740. doi:10.1038/aps.2013.27
53. Eyler CE, Rich JN. Survival of the fittest: cancer stem cells in therapeutic resistance and angiogenesis. *J Clin Oncol*. 2008;26(17):2839-2845. doi:10.1200/JCO.2007.15.1829
54. Bao S, Wu Q, McLendon RE, et al. Glioma stem cells promote radioresistance by preferential activation of the DNA damage response. *Nature*. 2006;444(7120):756-760. doi:10.1038/nature05236
55. Hirschmann-Jax C, Foster AE, Wulf GG, et al. A distinct "side population" of cells with high drug efflux capacity in human tumor cells. *Proc Natl Acad Sci U S A*. 2004;101(39):14228-14233. doi:10.1073/pnas.0400067101
56. Lee G, R Hall R, Ahmed AU. Cancer Stem Cells: Cellular Plasticity, Niche, and its Clinical Relevance. *J Stem Cell Res Ther*. 2016;06(10). doi:10.4172/2157-7633.1000363
57. Peitzsch C, Tyutyunnykova A, Pantel K, Dubrovskaya A. Cancer stem cells: The root of tumor recurrence and metastases. *Semin Cancer Biol*. 2017;44:10-24. doi:10.1016/j.semcancer.2017.02.011
58. Schatton T, Frank NY, Frank MH. Identification and targeting of cancer stem cells. *BioEssays*. 2009;31(10):1038-1049. doi:10.1002/bies.200900058
59. Hu Y, Smyth GK. ELDA: extreme limiting dilution analysis for comparing depleted and enriched populations in stem cell and other assays. *J Immunol Methods*. 2009;347(1-2):70-78. doi:10.1016/j.jim.2009.06.008
60. Visvader JE. Cells of origin in cancer. *Nature*. 2011;469(7330):314-322. doi:10.1038/nature09781

61. Chaffer CL, Weinberg RA. How Does Multistep Tumorigenesis Really Proceed? *Cancer Discov.* 2015;5(1):22-24. doi:10.1158/2159-8290.CD-14-0788
62. Liu J, Xiao Z, Wong SK-M, et al. Lung cancer tumorigenicity and drug resistance are maintained through ALDHhi/CD44hi tumor initiating cells. *Oncotarget.* 2013;4(10). doi:10.18632/oncotarget.1246
63. Jolly MK, Boareto M, Huang B, et al. Implications of the hybrid epithelial/mesenchymal phenotype in metastasis. *Front Oncol.* 2015;5(Jun). doi:10.3389/fonc.2015.00155
64. Nieto MA, Huang RYYJ, Jackson RAA, Thiery JPP. EMT: 2016. *Cell.* 2016;166(1):21-45. doi:10.1016/j.cell.2016.06.028
65. Kim DH, Xing T, Yang Z, Dudek R, Lu Q, Chen Y-H. Epithelial Mesenchymal Transition in Embryonic Development, Tissue Repair and Cancer: A Comprehensive Overview. *J Clin Med.* 2017;7(1):1. doi:10.3390/jcm7010001
66. Huang RYJ, Wong MK, Tan TZ, et al. An EMT spectrum defines an anoikis-resistant and spheroidogenic intermediate mesenchymal state that is sensitive to e-cadherin restoration by a src-kinase inhibitor, saracatinib (AZD0530). *Cell Death Dis.* 2013;4(11). doi:10.1038/cddis.2013.442
67. Grosse-Wilde A, Fouquier d'Hérouël A, McIntosh E, et al. Stemness of the hybrid Epithelial/Mesenchymal State in Breast Cancer and Its Association with Poor Survival. *PLoS One.* 2015;10(5):e0126522. doi:10.1371/journal.pone.0126522
68. Andriani F, Bertolini G, Facchinetti F, et al. Conversion to stem-cell state in response to microenvironmental cues is regulated by balance between epithelial and mesenchymal features in lung cancer cells. *Mol Oncol.* 2016;10(2):253-271. doi:10.1016/j.molonc.2015.10.002
69. Dick JE. Breast cancer stem cells revealed. *Proc Natl Acad Sci.* 2003;100(7):3547-3549. doi:10.1073/pnas.0830967100
70. Bisson I, Prowse DM. WNT signaling regulates self-renewal and differentiation of prostate cancer cells with stem cell characteristics. *Cell Res.* 2009;19(6):683-697. doi:10.1038/cr.2009.43
71. Dontu G, Jackson KW, McNicholas E, Kawamura MJ, Abdallah WM, Wicha MS. Role of Notch signaling in cell-fate determination of human mammary stem/progenitor cells. *Breast Cancer Res.* 2004;6(6):R605-15. doi:10.1186/bcr920
72. Hernandez-Vargas H, Ouzounova M, Le Calvez-Kelm F, et al. Methylome analysis reveals Jak-STAT pathway deregulation in putative breast cancer stem cells. *Epigenetics.* 2011;6(4):428-439. doi:10.4161/epi.6.4.14515

73. Tai M-H, Chang C-C, Kiupel M, Webster JD, Olson LK, Trosko JE. Oct4 expression in adult human stem cells: evidence in support of the stem cell theory of carcinogenesis. *Carcinogenesis*. 2004;26(2):495-502. doi:10.1093/carcin/bgh321
74. Liu K, Lin B, Zhao M, et al. The multiple roles for Sox2 in stem cell maintenance and tumorigenesis. *Cell Signal*. 2013;25(5):1264-1271. doi:10.1016/j.cellsig.2013.02.013
75. Eberle I, Pless B, Braun M, Dingermann T, Marschalek R. Transcriptional properties of human NANOG1 and NANOG2 in acute leukemic cells. *Nucleic Acids Res*. 2010;38(16):5384-5395. doi:10.1093/nar/gkq307
76. Malfettone A, Soukupova J, Bertran E, et al. Transforming growth factor- β -induced plasticity causes a migratory stemness phenotype in hepatocellular carcinoma. *Cancer Lett*. 2017;392:39-50. doi:10.1016/j.canlet.2017.01.037
77. Xie T, Mo L, Li L, et al. Identification of side population cells in human lung adenocarcinoma A549 cell line and elucidation of the underlying roles in lung cancer. *Oncol Lett*. 2018;15(4):4900-4906. doi:10.3892/ol.2018.7956
78. Zhang HZ, Lin XG, Hua P, et al. The study of the tumor stem cell properties of CD133+CD44+ cells in the human lung adenocarcinoma cell line A549. *Cell Mol Biol (Noisy-le-grand)*. 2010;56.
79. Shao C, Sullivan JP, Girard L, et al. Essential role of aldehyde dehydrogenase 1A3 for the maintenance of non-small cell lung cancer stem cells is associated with the STAT3 pathway. *Clin Cancer Res*. 2014;20(15):4154-4166. doi:10.1158/1078-0432.CCR-13-3292
80. Chen Y-C, Hsu H-S, Chen Y-W, et al. Oct-4 expression maintained cancer stem-like properties in lung cancer-derived CD133-positive cells. *PLoS One*. 2008;3(7):e2637. doi:10.1371/journal.pone.0002637
81. Qiu Y, Pu T, Guo P, et al. ALDH(+)/CD44(+) cells in breast cancer are associated with worse prognosis and poor clinical outcome. *Exp Mol Pathol*. 2016;100(1):145-150. doi:10.1016/j.yexmp.2015.11.032
82. Bhat KPL, Balasubramanian V, Vaillant B, et al. Mesenchymal Differentiation Mediated by NF- κ B Promotes Radiation Resistance in Glioblastoma. *Cancer Cell*. 2013;24(3):331-346. doi:10.1016/j.ccr.2013.08.001
83. Zhou Y, Xia L, Wang H, et al. Cancer stem cells in progression of colorectal cancer. *Oncotarget*. 2018;9(70):33403-33415. doi:10.18632/oncotarget.23607

84. Chen W, Zhang X, Chu C, et al. Identification of CD44+ cancer stem cells in human gastric cancer. *Hepatogastroenterology*. 2013;60(124):949-954. doi:10.5754/hge12881
85. Black W, Vasiliou V. The Aldehyde Dehydrogenase Gene Superfamily Resource Center. *Hum Genomics*. 2009;4(2):136-142. doi:10.1186/1479-7364-4-2-136
86. Trager WF. Principles of Drug Metabolism 1: Redox Reactions. In: *Comprehensive Medicinal Chemistry II*. Elsevier; 2007:87-132. doi:10.1016/B0-08-045044-X/00119-X
87. Marcato P, Dean CA, Liu RZ, et al. Aldehyde dehydrogenase 1A3 influences breast cancer progression via differential retinoic acid signaling. *Mol Oncol*. 2015;9(1):17-31. doi:10.1016/j.molonc.2014.07.010
88. Cunningham TJ, Duester G. Mechanisms of retinoic acid signalling and its roles in organ and limb development. *Nat Publ Gr*. 2015;16. doi:10.1038/nrm3932
89. De The H, Del Mar Vivanco-Ruiz M, Tiollais P, Stunnenberg H, Dejean A. Identification of a retinoic acid responsive element in the retinoic acid receptor & beta. *Nature*. 1990;343(6254):177-180. doi:10.1038/343177a0
90. Ginestier C, Wicinski J, Cervera N, et al. Retinoid signaling regulates breast cancer stem cell differentiation. *Cell Cycle*. 2009;8(20):3297-3302. doi:10.4161/cc.8.20.9761
91. Gudas LJ, Wagner JA. Retinoids regulate stem cell differentiation. *J Cell Physiol*. 2011;226(2):322-330. doi:10.1002/jcp.22417
92. Miyake K, Kincade PW. A new cell adhesion mechanism involving hyaluronate and CD44. *Curr Top Microbiol Immunol*. 1990;166:87-90. doi:10.1007/978-3-642-75889-8_12
93. Yu Q, Stamenkovic I. Localization of matrix metalloproteinase 9 to the cell surface provides a mechanism for CD44-mediated tumor invasion. *Genes Dev*. 1999;13(1):35-48. doi:10.1101/gad.13.1.35
94. Nakayama Y, Okazaki K, Shibao K, et al. Alternative expression of the collagenase and adhesion molecules in the highly metastatic clones of human colonic cancer cell lines. *Clin Exp Metastasis*. 1998;16(5):461-469.
95. Weber GF, Ashkar S, Cantor H. Interaction between CD44 and osteopontin as a potential basis for metastasis formation. *Proc Assoc Am Physicians*. 1997;109(1):1-9.

96. Senbanjo LT, Chellaiah MA. CD44: A multifunctional cell surface adhesion receptor is a regulator of progression and metastasis of cancer cells. *Front Cell Dev Biol.* 2017;5(MAR). doi:10.3389/fcell.2017.00018
97. Zhang H, Brown RL, Wei Y, et al. CD44 splice isoform switching determines breast cancer stem cell state. *Genes Dev.* 2019;33(3-4):166-179. doi:10.1101/gad.319889.118
98. Nishino M, Ozaki M, Hegab AE, et al. Variant CD44 expression is enriching for a cell population with cancer stem cell-like characteristics in human lung adenocarcinoma. *J Cancer.* 2017;8(10):1774-1785. doi:10.7150/jca.19732
99. Stoolmiller A, Dorfman A. The biosynthesis of hyaluronic acid. *J Biol Chem.* 1969;244(2):236-246. doi:10.1016/S0096-5332(08)60211-8
100. Cyphert JM, Trempus CS, Garantziotis S. Size Matters: Molecular Weight Specificity of Hyaluronan Effects in Cell Biology. *Int J Cell Biol.* 2015;2015:563818. doi:10.1155/2015/563818
101. Takabe P, Bart G, Ropponen A, et al. Hyaluronan synthase 3 (HAS3) overexpression downregulates MV3 melanoma cell proliferation, migration and adhesion. *Exp Cell Res.* 2015;337(1):1-15. doi:10.1016/j.yexcr.2015.07.026
102. Deed R, Rooney P, Kumar P, et al. Early-response gene signalling is induced by angiogenic oligosaccharides of hyaluronan in endothelial cells. Inhibition by non-angiogenic, high-molecular-weight hyaluronan. *Int J cancer.* 1997;71(2):251-256. doi:10.1002/(sici)1097-0215(19970410)71:2<251::aid-ijc21>3.0.co;2-j
103. Enegd B, King JAJ, Stylli S, et al. Overexpression of hyaluronan synthase-2 reduces the tumorigenic potential of glioma cells lacking hyaluronidase activity. *Neurosurgery.* 2002;50(6):1311-1318. doi:10.1097/00006123-200206000-00023
104. Yu M, He P, Liu Y, et al. Hyaluroan-regulated lymphatic permeability through S1P receptors is crucial for cancer metastasis. *Med Oncol.* 2015;32(1):1-8. doi:10.1007/s12032-014-0381-1
105. Tan J-X, Wang X-Y, Su X-L, et al. Upregulation of HYAL1 Expression in Breast Cancer Promoted Tumor Cell Proliferation, Migration, Invasion and Angiogenesis. Chammas R, ed. *PLoS One.* 2011;6(7):e22836. doi:10.1371/journal.pone.0022836
106. Törrönen K, Nikunen K, Kärnä R, Tammi M, Tammi R, Rilla K. Tissue distribution and subcellular localization of hyaluronan synthase isoenzymes. *Histochem Cell Biol.* 2014;141(1):17-31. doi:10.1007/s00418-013-1143-4

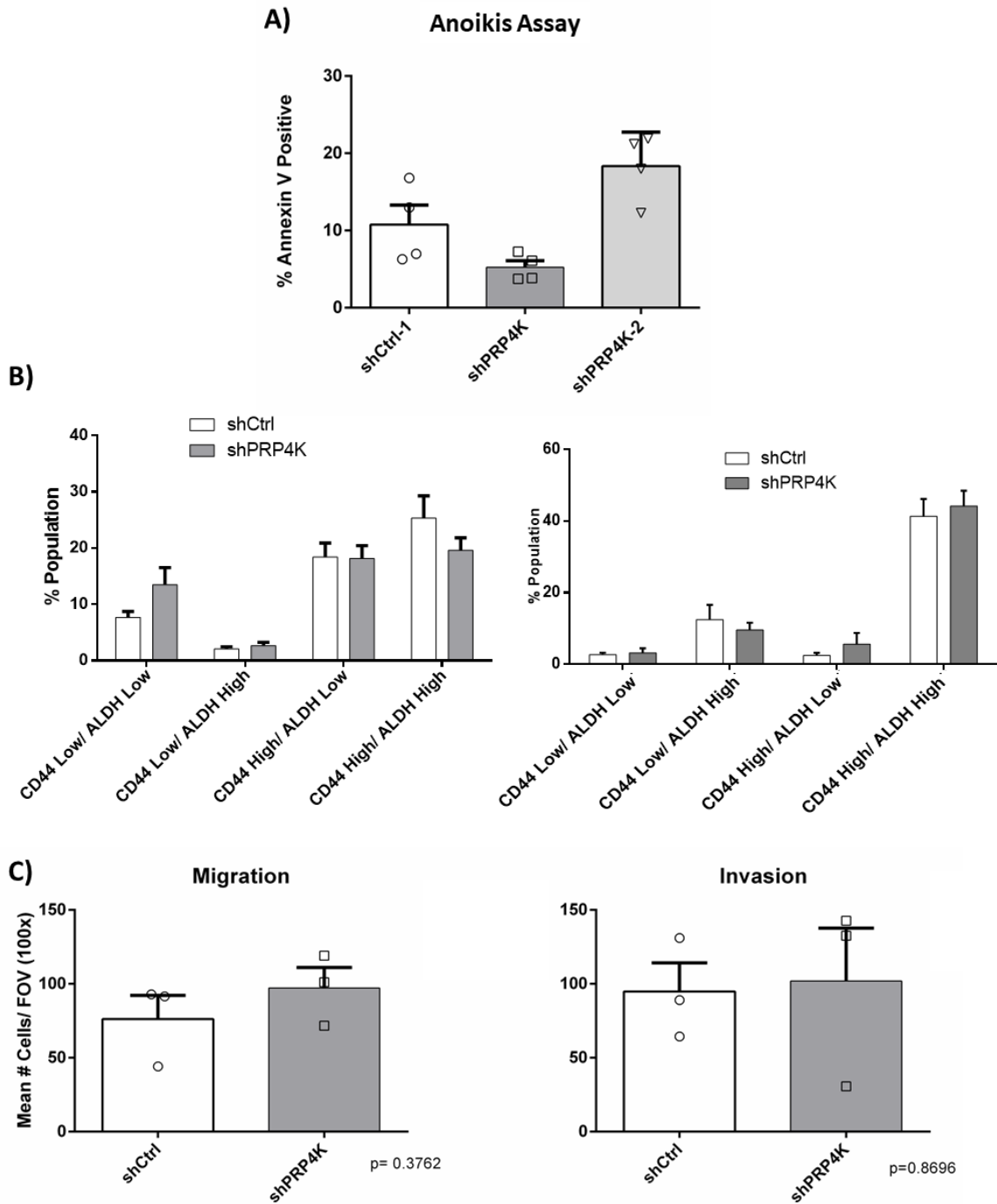
107. Liu M, Tolg C, Turley E. Dissecting the dual nature of hyaluronan in the tumor microenvironment. *Front Immunol.* 2019;10(May). doi:10.3389/fimmu.2019.00947
108. Kakizaki I, Kojima K, Takagaki K, et al. A novel mechanism for the inhibition of hyaluronan biosynthesis by 4-methylumbelliferone. *J Biol Chem.* 2004;279(32):33281-33289. doi:10.1074/jbc.M405918200
109. Kultti A, Pasonen-Seppänen S, Jauhiainen M, et al. 4-Methylumbelliferone inhibits hyaluronan synthesis by depletion of cellular UDP-glucuronic acid and downregulation of hyaluronan synthase 2 and 3. *Exp Cell Res.* 2009;315(11):1914-1923. doi:10.1016/j.yexcr.2009.03.002
110. Nagy N, Kuipers HF, Frymoyer AR, et al. 4-Methylumbelliferone treatment and hyaluronan inhibition as a therapeutic strategy in inflammation, autoimmunity, and cancer. *Front Immunol.* 2015;6(Mar). doi:10.3389/fimmu.2015.00123
111. Lokman NA, Price ZK, Hawkins EK, Macpherson AM, Oehler MK, Ricciardelli C. 4-Methylumbelliferone Inhibits Cancer Stem Cell Activation and Overcomes Chemoresistance in Ovarian Cancer. *Cancers (Basel).* 2019;11(8):1187. doi:10.3390/cancers11081187
112. Sukowati CHC, Anfuso B, Fiore E, et al. Hyaluronic acid inhibition by 4-methylumbelliferone reduces the expression of cancer stem cells markers during hepatocarcinogenesis. *Sci Rep.* 2019;9(1). doi:10.1038/s41598-019-40436-6
113. Dellaire G, Makarov EM, Cowger JJM, et al. Mammalian PRP4 kinase copurifies and interacts with components of both the U5 snRNP and the N-CoR deacetylase complexes. *Mol Cell Biol.* 2002;22(14):5141-5156.
114. Schneider M, Hsiao H-H, Will CL, Giet R, Urlaub H, Lührmann R. Human PRP4 kinase is required for stable tri-snRNP association during spliceosomal B complex formation. *Nat Struct Mol Biol.* 2010;17(2):216-221. doi:10.1038/nsmb.1718
115. Montembault E, Dutertre S, Prigent C, Giet R. PRP4 is a spindle assembly checkpoint protein required for MPS1, MAD1, and MAD2 localization to the kinetochores. *J Cell Biol.* 2007;179(4):601-609. doi:10.1083/jcb.200703133
116. Lahsaee S, Corkery DP, Anthes LE, Holly A, Dellaire G. Estrogen receptor alpha (ESR1)-signaling regulates the expression of the taxane-response biomarker PRP4K. *Exp Cell Res.* 2016;340(1):125-131. doi:10.1016/j.yexcr.2015.12.013
117. Corkery D, Clarke L, Gebremeskel S, et al. Loss of PRP4K drives anoikis resistance in part by dysregulation of epidermal growth factor receptor endosomal trafficking. *Oncogene.* 2018;37:174-184. doi:10.1038/onc.2017.318

118. Moreb JS, Zucali JR, Ostmark B, Benson NA. Heterogeneity of aldehyde dehydrogenase expression in lung cancer cell lines is revealed by Aldefluor flow cytometry-based assay. *Cytometry B Clin Cytom.* 2007;72(4):281-289. doi:10.1002/cyto.b.20161
119. Hellemans J, Mortier G, De Paepe A, Speleman F, Vandesompele J. qBase relative quantification framework and software for management and automated analysis of real-time quantitative PCR data. *Genome Biol.* 2007;8(2):R19. doi:10.1186/gb-2007-8-2-r19
120. Corkery DP, Le Page CÉc, Meunier L, Provencher D, Masson AMM, Dellaire G. Prp4k is a her2-regulated modifier of taxane sensitivity. *Cell Cycle.* 2014;14(7):1059-1069. doi:10.1080/15384101.2015.1007775
121. Gyorffy B, Surowiak P, Budczies J, Lánczky A. Online survival analysis software to assess the prognostic value of biomarkers using transcriptomic data in non-small-cell lung cancer. *PLoS One.* 2013;8(12):e82241. doi:10.1371/journal.pone.0082241
122. Duan Z, Weinstein EJ, Ji D, et al. Lentiviral short hairpin RNA screen of genes associated with multidrug resistance identifies PRP-4 as a new regulator of chemoresistance in human ovarian cancer. *Mol Cancer Ther.* 2008;7(8):2377-2385. doi:10.1158/1535-7163.MCT-08-0316
123. Cho YS, Zhu J, Li S, Wang B, Han Y, Jiang J. Regulation of Yki/Yap subcellular localization and Hpo signaling by a nuclear kinase PRP4K. *Nat Commun.* 2018;9(1). doi:10.1038/s41467-018-04090-2
124. Koedoot E, Fokkelman M, Rogkoti VM, et al. Uncovering the signaling landscape controlling breast cancer cell migration identifies novel metastasis driver genes. *Nat Commun.* 2019;10(1). doi:10.1038/s41467-019-11020-3
125. Islam SU, Ahmed MB, Lee SJ, et al. PRP4 kinase induces actin rearrangement and epithelial-mesenchymal transition through modulation of the actin-binding protein cofilin. 2018. doi:10.1016/j.yexcr.2018.05.018
126. Gao Q, Mechin I, Kothari N, et al. Evaluation of cancer dependence and druggability of PRP4 kinase using cellular, biochemical, and structural approaches. *J Biol Chem.* 2013;288(42):30125-30138. doi:10.1074/jbc.M113.473348
127. Ben-David U, Siranosian B, Ha G, et al. Genetic and transcriptional evolution alters cancer cell line drug response. doi:10.1038/s41586-018-0409-3

128. Herreros-Pomares A, de-Maya-Girones JD, Calabuig-Fariñas S, et al. Lung tumorspheres reveal cancer stem cell-like properties and a score with prognostic impact in resected non-small-cell lung cancer. *Cell Death Dis.* 2019;10(9):1-14. doi:10.1038/s41419-019-1898-1
129. Persaud SD, Park SW, Ishigami-Yuasa M, Koyano-Nakagawa N, Kagechika H, Wei LN. All trans-retinoic acid analogs promote cancer cell apoptosis through non-genomic Crabp1 mediating ERK1/2 phosphorylation. *Sci Rep.* 2016;6. doi:10.1038/srep22396
130. Favorskaya I, Kainov Y, Chemeris G, Komelkov A, Zborovskaya I, Tchevkina E. Expression and clinical significance of CRABP1 and CRABP2 in non-small cell lung cancer. doi:10.1007/s13277-014-2348-4
131. Yang Q, Wang R, Xiao W, Sun F, Yuan H, Pan Q. Cellular retinoic acid binding protein 2 is strikingly downregulated in human esophageal squamous cell carcinoma and functions as a tumor suppressor. *PLoS One.* 2016;11(2):e0148381. doi:10.1371/journal.pone.0148381
132. Feng X, Zhang M, Wang B, et al. CRABP2 regulates invasion and metastasis of breast cancer through hippo pathway dependent on ER status. *J Exp Clin Cancer Res.* 2019;38(1):361. doi:10.1186/s13046-019-1345-2
133. Chisholm DR, Tomlinson CWE, Zhou GL, et al. Fluorescent Retinoic Acid Analogues as Probes for Biochemical and Intracellular Characterization of Retinoid Signaling Pathways. *ACS Chem Biol.* 2019;14(3):369-377. doi:10.1021/acscchembio.8b00916
134. Konermann S, Lotfy P, Brideau NJ, Oki J, Shokhirev MN, Hsu PD. Transcriptome Engineering with RNA-Targeting Type VI-D CRISPR Effectors. *Cell.* 2018;173(3):665-676.e14. doi:10.1016/j.cell.2018.02.033
135. Hart T, Chandrashekhar M, Aregger M, et al. High-Resolution CRISPR Screens Reveal Fitness Genes and Genotype-Specific Cancer Liabilities. *Cell.* 2015;163(6):1515-1526. doi:10.1016/j.cell.2015.11.015
136. Nishimura K, Fukagawa T, Takisawa H, Kakimoto T, Kanemaki M. An auxin-based degron system for the rapid depletion of proteins in nonplant cells. *Nat Methods.* 2009;6(12):917-922. doi:10.1038/nmeth.1401
137. Tan X, Calderon-Villalobos LIA, Sharon M, et al. Mechanism of auxin perception by the TIR1 ubiquitin ligase. *Nature.* 2007;446(7136):640-645. doi:10.1038/nature05731

138. Li S, Prasanna X, Salo VT, Vattulainen I, Ikonen E. An efficient auxin-inducible degron system with low basal degradation in human cells. *Nat Methods*. 2019;16(9):866-869. doi:10.1038/s41592-019-0512-x
139. Franks LM, Carbonell AW, Hemmings VJ, Riddle PN. Metastasizing tumors from serum-supplemented and serum-free cell lines from a C57BL mouse lung tumor. *Cancer Res*. 1976;36(3):1049-1055.
140. Agalioti T, Giannou AD, Krontira AC, et al. Mutant KRAS promotes malignant pleural effusion formation. *Nat Commun*. 2017;8. doi:10.1038/ncomms15205
141. Justilien V, Regala RP, Tseng IC, et al. Matrix metalloproteinase-10 is required for lung cancer stem cell maintenance, tumor initiation and metastatic potential. *PLoS One*. 2012;7(4). doi:10.1371/journal.pone.0035040

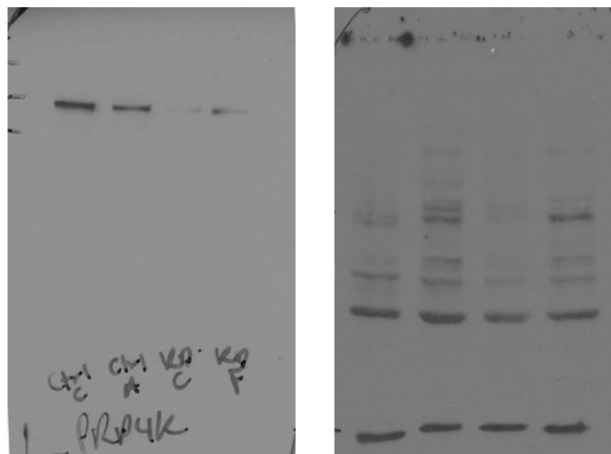
Appendix 1



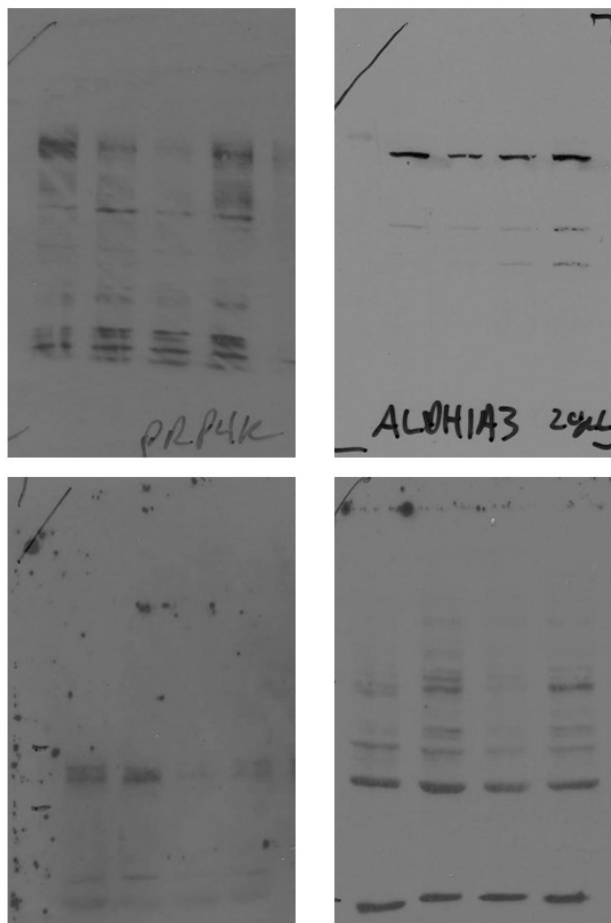
Appendix 1 PRP4K knockdown had no effect on certain *in vitro* assays. (A) One PRP4K KD line conferred resistance to anoikis, but the other did not; **(B)** PRP4K KD did not affect the distribution of CSC populations in LLCs; **(C)** PRP4K KD did not affect migration (left) or invasion (right).

Appendix 2

3.1.2B Full Length Blots (PRP4K, Tubulin)

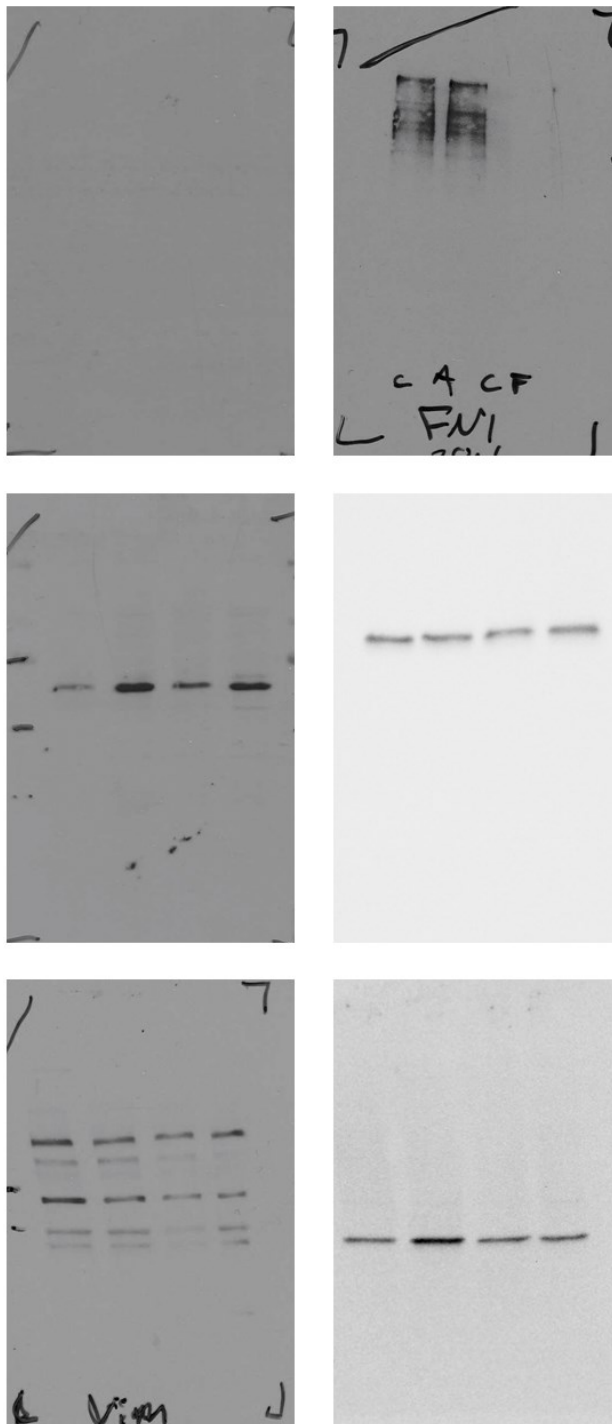


3.1.5 Full Length Blots (PRP4K, ALDH1A3, CD44, Tubulin)



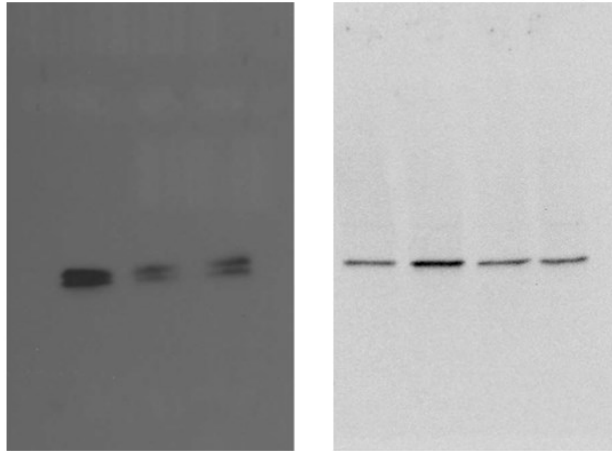
Appendix 2 Cont'd

3.1.7 Full Length Blots (CDH1, FN1, Snail, Slug, Vim, Tubulin)



Appendix 2 Cont'd

3.1.9 Full Length Blots (Crabp1, Tubulin)



Appendix 7 Full Length Blots (Crabp1, Lamin B, total protein)

